General Disclaimer

One or more of the Following Statements may affect this Document

- This document has been reproduced from the best copy furnished by the organizational source. It is being released in the interest of making available as much information as possible.

- This document may contain data, which exceeds the sheet parameters. It was furnished in this condition by the organizational source and is the best copy available.

- This document may contain tone-on-tone or color graphs, charts and/or pictures, which have been reproduced in black and white.

- This document is paginated as submitted by the original source.

- Portions of this document are not fully legible due to the historical nature of some of the material. However, it is the best reproduction available from the original submission.

Radiance, Polarization, and Ellipticity of the Radiation in the Earth's Atmosphere

By

Stephen J. Hitzfelder, Gilbert N. Plass,

and George W. Kattawar

Department of Physics
Texas A&M University
College Station, Texas 77843

Report No. 24

The research described in this report was

funded by the

National Aeronautics and Space Administration

Contract No. NGR 44-001-117

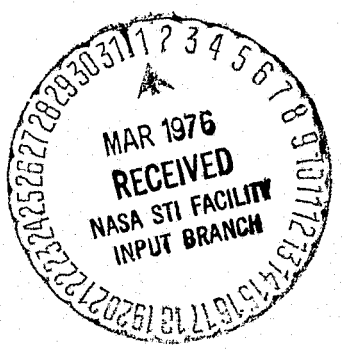

Department of Physics
Texas A&M University
College Station, Texas 77843

February 2, 1976

A paper based on the material in this report has been submitted to Applied Optics.

Radiance, Polarization, and Ellipticity of the Radiation in the Earth's Atmosphere

By

Stephen J. Hitzfelder, Gilbert N. Plass, and George W. Kattawar

The complete radiation field including polarization is calculated for a model of the real atmosphere by the matrix operator method. The radiance, direction and amount of polarization, and ellipticity are obtained at the top and bottom of the atmosphere for three values of the surface albedo (0; 0.15; 0.90) and five solar zenith angles. Scattering and absorption by molecules (including ozone) and by aerosols are taken into account together with the variation of the number density of these substances with height. All results are calculated for both a normal aerosol number and a distribution which is one-third of the normal amount at all heights. The calculated values show general qualitative agreement with the available experimental measurements. The position of the neutral points of the polarization in the principal plane is a sensitive indicator of the characteristics of the aerosol particles in the atmosphere, since it depends on the sign and value of the single scattered polarization for scattering angles around 20° and 160° for transmitted and reflected photons respectively. This in turn depends on the index of refraction and size distribution of the aerosols. The neutral point position does not depend appreciably on the surface albedo and, over a considerable range, depends little on the solar zenith angle. The value of the maximum polarization in the principal plane depends on the aerosol amount, surface albedo, and solar zenith angle. It could be used to measure the aerosol amount. The details of the ellipticity curves are very similar to those for scattering from pure aerosol layers and thus are little modified by the Rayleigh scattering. Aerosols could be identified by their characteristic ellipticity curves.

The authors are with the Physics Department, Texas A&M University, College Station, Texas 77843.

I. Introduction

A complete description of the radiation field scattered from or transmitted through an atmospheric layer requires a specification of the degree and direction of polarization and the ellipticity of the radiation in addition to the radiance. Even though the incoming solar radiation is unpolarized to a high approximation, the multiple scattered light in a planetary atmosphere is in general polarized.

Elegant and elaborate mathematical solutions have been developed to calculate the scattering from layers with isotropic and Rayleigh phase functions. These methods together with calculated results have been reviewed recently by Kattawar et al[1] (referred to hereafter as I). They also discuss the more general methods including Monte Carlo, iterative, doubling and matrix operator that have been used in recent years for the solution of problems with phase functions applicable to hazes and clouds of various types. The radiance, polarization, and neutral points of the multiple scattered radiation emerging from continental haze layers is given in I, while the ellipticity and direction of polarization of this radiation is given by Plass et al[2] (referred to hereafter as II). These results are all for layers of uniform composition.

The actual atmosphere is highly inhomogeneous with the number of molecules and aerosols varying in a different manner with height. Relatively few studies have attempted to calculate the polarization and ellipticity of the radiation using a realistic model for the vertical variations of the components of the earth's atmosphere. The only two studies of which we are aware are those of Plass and Kattawar[3] by the Monte Carlo method and Tanaka[4] by a matrix method.

The matrix operator method has been modified in the present study so that the complete radiation field can be calculated from a realistic model of the earth's atmosphere. The results are compared with those previously reported in I and II for Rayleigh and continental haze layers.

II. Computational Aspects and Atmospheric Model

Atmospheric models that included only Rayleigh, but not aerosol scattering, were studied by Sekera[5] and others. Their results clearly indicate that the scattering and absorption of the radiation by the aerosols as well as ozone absorption must be included in a realistic model in addition to the Rayleigh scattering. Our model includes these factors.

The extinction coefficients for the Rayleigh, aerosol, and ozone constituents as a function of height are taken from the tables given by Elterman et al[6]. Two different models were derived from his data: the unchanged or normal model in which the aerosol amount as a function of height agrees with Elterman's tables and the one-third normal model, in which the aerosol constituent was reduced to one-third the normal amount at each height, while the other atmospheric constituents were kept unchanged. These two models were used to study the effects of varying the aerosol content of the earth's atmosphere. The data used from Elterman's tables was for a wavelength of 0.55 μm, in the middle of the visible region. For the normal model, the total optical depth was 0.378; for the one-third normal model, the total optical depth was 0.212. The one-third normal model has a different effective phase matrix as well as a different total optical depth than the normal model. Both of these differences have an important influence on the calculated results.

The aerosols were represented by the haze L model for the continental haze proposed by Deirmenjian[7]. The number of particles with a given radius is proportional to $r^2 \exp(-15.1186 r^{1/2})$, where r is the particle radius. The mode radius is 0.07 μm. At the wavelength of 0.55 μm, the real and imaginary parts of the index of refraction for the aerosols were assumed to be $n_1 = 1.55$ and $n_2 = 0.05$.

The single scattering phase matrix for haze L was calculated by the method described by Kattawar and Plass[8] and Kattawar et al[9]. The Mie scattering matrix was obtained for size parameters $x = 2\pi r/\lambda$ from 0.05 to 30 using a 50th order Gauss

quadrature. The calculated single scattering albedo is 0.7171. Fifty-five Fourier terms were used to describe the phase matrix. The single scattering function obtained from this phase matrix is shown in Fig. 5 of I. There is a fairly strong maximum in the backward direction (the glory) and a slight maximum at the rainbow angle. The value at the minimum is about 1/300 of that in the forward direction.

The surface of the earth has a considerable effect on both the radiance and polarization. Although it is not realistic, the earth's surface is represented by a Lambert surface which reflects radiation uniformly into all available solid angles and completely depolarizes the radiation on reflection. Three values of the surface albedo are considered, A = 0, 0.15, and 0.90. The zero value is considered for two reasons: it is easy to calculate and, when compared with other results, it helps to demonstrate the effect of a real surface on the reflected and transmitted radiation. A reasonable average value for the albedo of the various surfaces on the earth is 0.15. Since a snow covered surface closely approximates a Lambert surface with an albedo of about 0.9, this value was also included in the calculations.

The complete multiple scattered radiation field was calculated by matrix operator theory as described in I and II and by Plass et al[10]. There is no difficulty in this formulation of the theory in applying it to atmospheres with vertical inhomogenieties. The atmosphere was initially divided into twenty layers each with appropriate average values for the Rayleigh, aerosol, and ozone scattering and absorbing coefficients. A different effective phase matrix was computed for each atmospheric layer from the haze L and Rayleigh phase matrices from the proportion of the two types of particles in the layer.

The calculation proceeded in the following way: the twenty layers were selected to have equal optical thickness. A single integration was performed for each layer with the Runge-Kutta method to obtain the reflection and transmission matrices at an optical thickness of 2^{-7}. This result was then doubled until the optical

thickness of the layer was achieved. This proceedure was repeated for each layer. The combining algorithm[10] was used to calculate the reflection and transmission matrices for the combination of two layers. This process was repeated until the reflection and transmission operators for the entire atmosphere had been constructed. The Lambert surface at the bottom of the atmosphere is easily included as a special case of the combining algorithm[10]. A 28 point Lobatto quadrature was used for the points and weights needed in the calculation.

The polarization is defined as

$$P = (Q^2 + U^2 + V^2)^{1/2}/I, \tag{1}$$

where the four components of the Stokes vector are taken as I, Q, U, V. In some cases it is desirable to assign a sign to the polarization which depends on whether I_r (perpendicular component of radiance) is greater or less than I_l (parallel component). Unfortunately both possible choices of sign have been used in the literature. Chandrasekhar[11] and I assign a negative sign to the polarization when $I_r > I_l$. Tanaka[4] and Coulson et al[12] assign a positive sign to the polarization when $I_r < I_l$. In this article we adopt the latter convention, so that our results can be compared more readily with those previously calculated for a real atmosphere by Tanaka. The polarization of radiation scattered by a Rayleigh phase function has a positive sign according to this convention.

III. Radiance

The transmitted diffuse radiance at the earth's surface as calculated from our model atmospheres is shown in Fig. 1 when the sun is at the zenith ($\Theta_0 = 0°$). Curves are shown for the model with a normal aerosol amount as well as the one with one-third of the normal amount. Results are given for both models for three surface albedos (A = 0, 0.15 and 0.90). In addition the radiance due to photons that have undergone only a single scattering event is shown for the normal aerosol model. The incoming solar flux is normalized to unity through a plane perpendicular to the

solar direction in this article. The transmitted radiance is always for the diffuse component only, i. e. photons that have undergone at least one scattering event.

The radiance transmitted through the atmosphere for A = 0 is greater for the normal aerosol model than for the one-third normal model except near the horizon, in agreement with the results of Plass and Kattawar[3]. There is horizon brightening for the one-third normal atmosphere in this case, while the radiance shows a maximum near 80° and then decreases toward the horizon for the normal atmosphere. This is connected with the fact that the transmitted radiation through a pure Rayleigh atmosphere shows horizon brightening up to an optical depth of about 0.5 and horizon darkening at greater optical depths (see Fig. 2 of I, and Coulson et al[12]). The radiance of the model atmospheres shows a much greater variation with the zenith angle of observation than in the case of Rayleigh scattering (Fig. 2 of I).

The transmitted radiance in the principal plane (ϕ = 0° and 180°) for various solar zenith angles (Θ_0 = 0°, 21.10°, 40.88°, 60.53°, 80.18°) is given in Fig. 2 when A = 0.15 and for the normal aerosol model. The diffuse radiance for directions near the solar position is very similar over this wide range of solar angles. The value of the radiance at the minimum decreases and the position of the minimum approaches the zenith as the sun approaches the horizon.

The reflected radiance as observed at the top of the atmosphere is shown in Fig. 3 when the sun is at the zenith. When A = 0, there is horizon darkening when the normal aerosol model is used and horizon brightening with the one-third normal model. Again this is connected with the fact that, in the case of Rayleigh scattering, there is horizon brightening through optical depths of 0.25 and horizon darkening at greater optical depths (see Fig. 1 of I, and Coulson et al[12]). The slight increase in the radiance for the normal atmosphere model at the nadir is due to the glory in the aerosol phase function.

The ground albedo exerts a much greater effect on the reflected radiance than the transmitted. The reflected radiance varies relatively little with nadir angle when A = 0.15 and 0.90. A comparison of the two atmospheric models yields an interesting point. When A = 0, the radiance is greater at most angles for the normal aerosol model than for the one-third normal model. On the other hand the one-third normal model radiance is the greater for the non-zero albedo cases. The reason is that the total downward flux (diffuse plus direct solar beam) is greater for the one-third than for the normal aerosol model. When the albedo is non-zero, this extra contribution after reflection from the earth's surface makes the reflected radiance at the top of the atmosphere greater for the one-third than for the normal model. On the other hand when the surface albedo is zero, the additional optical thickness of the normal atmosphere model over the one-third normal one provides additional scattering centers to increase the radiance (except near the horizon where the effective optical thickness is already large).

The reflected radiance for $\Theta_0 = 80.18°$ in the principal plane is given in Fig. 4. A comparison of the normal and one-third normal radiances reveals that they have the same relationship to each other as in Fig. 3 over a wide range of nadir angles, except near the horizon in many cases. Even when A = 0.90, the reflected radiance still exhibits a strong maximum near the solar horizon from the aerosol phase function; the reflected radiation from the ground is not strong enough even in this case to smooth out the variation of the radiance with nadir angle, as it does when the sun is at the zenith.

The reflected radiance is shown in Fig. 5 for five solar zenith angles when A = 0.15 and for two solar zenith angles when A = 0. These results are for the normal aerosol model and are given in the principal plane ($\phi = 0°$ and 180°). The ground albedo has a much more important effect on the reflected radiance when $\Theta_0 = 0°$ than when $\Theta_0 = 80.18°$. When the sun is at the zenith, the reflected radiance varies little

with nadir angle when A = 0.15. As the sun moves toward the horizon, the reflected radiance shows a greater variation with nadir angle, until there is a deep minimum near the nadir and a large maximum at the solar horizon when $\Theta_0 = 80.18°$.

IV. Polarization

The polarization was calculated from the four components of the Stokes vector according to Eq. (1) and with the sign convention explained thereafter. The single scattered polarization for the haze L aerosols assumed for the model atmospheres is shown in Fig. 18 of I. The sign of the results shown in this figure should be changed when comparing the results with the present article.

The polarization of the transmitted photons is shown in Fig. 6 for the normal aerosol model and for A = 0.15. Curves are given for $\Theta_0 = 0°$, 21.20°, 40.88°, 60.53°, 80.18° in the principal plane. The maximum value for the polarization occurs very roughly at right angles to the solar direction; this feature is strongly influenced by the polarization resulting from Rayleigh type scattering events, but it is modified by the presence of the aerosols. The polarization is positive at most zenith angles, but does become weakly negative over certain small regions well away from the maxima. These calculated results agree very well in general shape and magnitude with the results measured by Coulson[13] for a relatively clear atmosphere in Los Angeles (see Fig. 1 of Coulson).

The polarization of the transmitted photons when the sun is at the zenith is shown in Fig. 7 for the two aerosol models and the three surface albedos. The polarization is larger at all angles for the one-third normal aerosol model than for the normal model. The reason for this is two fold. First, the optical depth is smaller for the one-third normal atmosphere. In general, the polarization increases toward the single scattering value as the optical depth decreases. The second effect depends on the behavior of the single scattering polarization itself. Since the aerosol single scattering polarization has the opposite sign to the Rayleigh single

scattering polarization at most angles, the value of the polarization tends to decrease as the aerosol amount increases. This is evident in the curves of Fig. 7, which also shows that the maximum tends to move toward the horizon as the aerosol amount decreases.

The polarization decreases as the surface albedo increases. This effect can be explained in the following manner. A Lambert surface acts as an isotropic, unpolarized source of radiation. If this were the only input source into the atmosphere, the radiation would be unpolarized everywhere in the atmosphere, since there is no preferred direction in space for this input function. When this radiation is added to that which develops from the solar beam without reflection from the bottom surface, the polarization necessarily decreases as the surface albedo increases. Although the surface albedo is expected to have a large effect on the polarization of the reflected radiation, it is interesting that it has as large an effect as that shown here for the polarization of the transmitted radiation.

The same polarization curves are given in Fig. 8, but for $\Theta_0 = 80.18°$ and in the principal plane ($\phi = 0°$ and $180°$). The surface albedo has less effect on the polarization when the sun is near the horizon than when it is at the zenith. A comparison of Fig. 8 with Fig. 16 of I shows that the neutral points are considerably changed from those for Rayleigh scattering. For the normal aerosol model the Babinet point (between solar direction and zenith) is 11.6° from the sun when A = 0 and the Arago point (near solar horizon) is 26.0° from the antisun (i. e. 16.2° from the solar horizon). The maximum polarization is about 0.601 and 0.778 for the one-third normal and normal aerosol models and occurs at approximately a 90° angle to the solar direction.

The angular distance from the neutral points to the solar direction is tabulated in Table I for five solar angles and three surface albedos. There are no neutral points for the transmitted radiation when the sun is at the zenith nor when $\Theta_0 =$

21.20° and A = 0.90 for the normal aerosol amount. The neutral points of the transmitted radiation change by only a few degrees as the surface albedo varies; the largest variation is at Θ_0 = 40.88°, when the Brewster point changes by 3.6° as the surface albedo varies from 0 to 0.90. As the aerosol amount changes from one-third normal to normal, the Brewster and Babinet points move closer to the solar direction; the largest changes for this variation in aerosol amount are 1.9° and 2.4° for the Brewster and Babinet points respectively. On the other hand, the Arago point for the transmitted radiation when Θ_0 = 80.18° moves away from the antisun as the aerosol amount increases; the largest change between the two tabulated aerosol amounts is 4.2° for the Arago point. The position of the Babinet and Brewster points of the transmitted radiation is relatively insensitive to the aerosol amount since the single scattered polarization of haze L is small for angles near the forward direction and thus has little influence in changing the polarization from that calculated for Rayleigh type scattering events only. The variation is larger near the Arago point, since a single scattered photon from haze L in the backward direction has relatively large and negative polarization.

The polarization of the transmitted radiation out of the principal plane is shown in Figs. 9 and 10 for Θ_0 = 80.18° and for the azimuthal angles ϕ = 60° and 120° and for ϕ = 90° respectively. Note that neutral points do not occur out of the principal plane. At most zenith angles the polarization increases as ϕ approaches 90°. The polarization curves at ϕ = 90°, given in Fig. 10, exhibit relatively little variation with zenith angle. For this solar zenith angle, the single scattering angle only varies between 80.1° and 90° in the ϕ = 90° plane; thus the single scattering always occurs near the 90° angle for maximum polarization from Rayleigh scattering events.

The polarization of the reflected photons is given in Fig. 11. Curves are given for five solar zenith angles, A = 0.15, ϕ = 0° and 180°, and normal aerosol amount. As expected the polarization is a maximum in each case at an angle approximately 90° to the solar direction.

The polarization for the reflected radiation is shown in Fig. 12, when the sun is at the zenith, for three surface albedos and the two aerosol models. The polarization of the reflected radiation is strongly influenced by the surface albedo. When A = 0.90, the polarization is appreciable only near the horizon. For the normal aerosol amount, there is a neutral point at approximately 20°, but none when the aerosol amount is one-third normal. There is no neutral point for a pure Rayleigh atmosphere with the sun at the zenith. A one-third normal aerosol atmosphere does not have sufficient aerosols to make the polarization negative near the nadir. However, when the normal aerosol model is used, the strong negative polarization for single scattering at angles near the backward direction characteristic of haze L (Fig. 18 of I; opposite sign convention used to present article) is sufficient so that there is a region of negative polarization from the nadir to approximately Θ = 20°. As the nadir angle further increases, the strong positive polarization from Rayleigh scattering dominates. Thus the neutral point for the reflected radiation is due to the interaction of the Rayleigh and haze L phase function. The position of this neutral point should thus be sensitive to the size distribution and index of refraction of the aerosols, since the single scattered polarization changes appreciably as these parameters are varied.

The polarization of the reflected photons when Θ_0 = 80.18° is shown in Fig. 13 in the principal plane for three surface albedos and the two aerosol models. The polarization is again strongly influenced by the surface albedo. On the other hand, the position of the Babinet neutral point approximately 22° from the antisun does not vary significantly with the surface albedo. The position of this neutral point is determined by interaction between the negative polarization produced for scattering from haze L at angles near the backward direction and the positive polarization from Rayleigh type scattering events. There are also Arago neutral points that are very close to the horizon and cannot be shown on the figure.

The polarization of the reflected photons for an intermediate solar angle, Θ_o = 40.88°, is given in Fig. 14. The curves in the region around the neutral points have been multiplied by 10 for clarity of presentation. The position of the neutral points changes appreciably as the aerosol amount is increased from one-third normal to normal. The dependence of the neutral point position on the surface albedo is small.

The single scattering polarization for the normal aerosol amount has neutral points very close to those calculated when multiple scattering is taken into account and in addition has the necessary neutral point in the direction of the antisun.

When A = 0, the polarization curves have maxima close to 42° and 46° for the normal and one-third normal models respectively. When A = 0.15 the curve for the normal model has a maximum near 66°, but the corresponding curve for the one-third normal model has a maximum at the horizon. The curves for the two models for A = 0.90 have maxima only at the horizon. In each case as the aerosol amount decreases, the polarization curve is approaching the one for a pure Rayleigh atmosphere with τ = 0.1 (nearly the optical thickness of the Rayleigh component of the atmosphere at 0.55 μm). For example, when A = 0, the maximum polarization is at a nadir angle of 48.3° for a pure Rayleigh atmosphere with τ = 0.1. When A $\geq$ 0.15, the maximum is at the antisolar horizon for Rayleigh scattering. This is the reason that the maximum moves from 66° for the normal aerosol amount to the horizon as the number of aerosols decreases.

The angular distance between the neutral points and the anti-solar direction is given in Table I for the reflected photons. There is a considerable variation in the position of these neutral points as the aerosol amount increases from one-third to normal, i. e. the angular distance of the Babinet point from the sun increases from 7.4° to 19.3° when Θ_o = 21.20° and A = 0. The position of these neutral points, as already discussed, should also be sensitive to the size distribution and index of

refraction of the aerosol particles. The position of the neutral points changes only slightly with the surface albedo; the largest change is at $\Theta_0 = 40.88°$ when the position of the Brewster point changes by 3.9° as the surface albedo varies from 0 to 0.90 for the one-third normal aerosol model.

The angle between the Babinet neutral point and the sun is shown in Fig. 15. For comparison the position of the Babinet point for a Rayleigh atmosphere of optical thickness 0.1 (nearly the actual value of the Rayleigh component of the atmosphere at 0.55 μm) is also shown in this figure. For $\Theta_0 > 25°$ the angle from the sun to the Babinet point for transmitted photons decreases as aerosols are added to a pure Rayleigh atmosphere, while the angle from the antisun for the reflected photons increases.

For the reflected photons a region of negative polarization develops around the antisun for finite pure Rayleigh scattering layers. The haze L particles have a strong negative polarization for scattering angles near 180°. Thus, as they are added to a Rayleigh layer, they increase the region of negative polarization and move the neutral points farther from the antisolar direction.

A pure Rayleigh layer of thickness 0.1 also develops a region of negative polarization around the direction of the transmitted solar beam. In this case haze L particles have a weak positive polarization for scattering angles from 3.53° to 25.6° (see Fig. 18 of I; change sign convention). Thus as aerosol particles are added to a Rayleigh layer, the region of negative polarization decreases and the neutral points move toward the solar direction. This also counteracts the movement of the Babinet point away from the sun as the optical thickness increases in this range.

The angle between the Brewster or Arago neutral points and the sun or antisun is given in Fig. 16 as a function of the solar zenith angle. When the solar zenith angle is between 0° and approximately 80° there is a Brewster neutral point (between sun or antisun and the horizon). When the solar zenith angle is approximately 80° the

Brewster neutral point touches the horizon; for greater solar zenith angles, there is an Arago neutral point (between antisolar horizon and zenith for transmitted photons and between solar horizon and nadir for reflected photons). The angle less than 90° from the neutral point to either the sun or antisun is plotted in Fig. 15. When this is done, the curves are continuous as the Brewster point changes into an Arago point.

As aerosols are added to a pure Rayleigh atmosphere, the Brewster point for the transmitted photons moves toward the sun, while that for the reflected photons moves away from the antisun. The explanation is identical with that given for the same behavior for the Babinet points. On the other hand, the Arago point moves away from the antisun for the transmitted photons and toward the sun for the reflected photons. The single scattered photons from the aerosols that are scattered into the direction of the Arago point for the transmitted photons have undergone approximately 160° scattering and thus have a strong negative polarization. This combines with the small region of negative polarization around the Arago point for a pure Rayleigh atmosphere, so that this region of negative polarization increases in angular width and thus moves the Arago point farther from the antisun. On the other hand, the single scattered photons from the aerosols that are scattered into the direction of the Arago point for the reflected photons have undergone approximately 20° scattering and have a weak positive polarization. This tends to decrease the angular width of the region of negative polarization that develops for pure Rayleigh scattering around the Arago point and thus the Arago point moves toward the sun as the aerosol amount increases.

All of the calculated results shown here assume haze L particles for the aerosols. Since the single scattering polarization is a sensitive function of the index of refraction and size distribution assumed for the aerosols, it follows that the various curves for the polarization and the location of the neutral points given here may be quite different for other types of particles.

Coulson[13] gives the variation of the Babinet point with sun elevation at 0.32 μm. The qualitative variation is the same as in our calculated Fig. 15, but the measured displacements are larger. This would be expected, since the Rayleigh optical thickness of the atmosphere is much larger at the measured wavelength and the Babinet point moves further from the sun as the optical thickness increases over this range (see I, Fig. 14 - 17).

Sekera et al[14] made a number of measurements of the positions of the neutral points. Although the results show considerable fluctuation from day to day and even from hour to hour, presumably due to aerosol variations, the results at 0.515 μm agree qualitatively with the present calculations for 0.55 μm. For example, at $\Theta_0 = 60°$ the measured position of the Brewster and Babinet points is 0° to 7° closer to the sun than the position calculated from a pure Rayleigh atmosphere. Our calculations for the Brewster and Babinet points for $\Theta_0 = 60°$ show that they are 2.8° and 2.8° respectively closer to the sun for the one-third normal aerosol model and 4.6° and 3.8° respectively closer for the normal aerosol model than the calculated values for a pure Rayleigh atmosphere.

When $\Theta_0 = 80°$, the measurements[14] of the position of the Arago point show that it is 4° to 7° farther from the antisun than the position calculated from a pure Rayleigh atmosphere. Our calculations for this case show a change of 4.0° and 8.2° for the one-third normal and normal aerosol models respectively. The Arago point must move away from the antisun as the aerosol amount increases for any aerosol whose single scattering polarization curve is strongly negative for scattering angles around 160°. For a different type of aerosol that has positive single scattering polarization values around this angle, the Arago point would move toward the antisun, as has occassionally been reported experimentally.

The maximum polarization in the principal plane as a function of solar zenith angle for three surface albedos and the two aerosol models is given in Fig. 17.

For comparison the curve is also shown for single scattering from the atmospheric model with normal aerosol amount. In general the maximum polarization of the transmitted photons increases or remains approximately constant as the solar zenith angle increases, while that for the reflected photons decreases at first to a minimum value and then increases as the sun nears the horizon; the minimum is quite pronounced when A = 0.15 and 0.90.

The zenith angle at which the maximum polarization is observed in the principal plane is shown in Fig. 18 as a function of the solar zenith angle. In all cases the maximum polarization for the transmitted photons is observed within 20° of the direction which is at right angles to the solar direction. No such rule holds for the reflected photons, as the maximum polarization is observed in many cases on the horizon.

The maximum polarization in the $\phi = 90°$ plane as a function of solar zenith angle is given in Fig. 19. At some angles the polarization is much larger than in the principal plane because the single scattering angle is nearer 90°.

Coulson[13] in Fig. 4 shows the maximum measured polarization at 0.55 μm in the principal plane dropping from about 0.6 for $\Theta_0 = 90°$ to 0.4 for $\Theta_0 = 30°$. This could be described well by our curve in Fig. 17 for the normal aerosol amount and a surface albedo a little greater than 0.15. Sekera et al[14] show this same quantity in Fig. 22 at 0.515 μm as measured at Cactus Peak, California decreasing from 0.8 at $\Theta_0 = 90°$ to 0.6 at $\Theta_0 = 15°$. This could be fitted by our calculations for the one-third normal aerosol model and A = 0.15. They also show the angular position of this maximum in Fig. 21; the distance from the sun is between 90° and about 92° for $15° < \Theta_0 < 80°$ at 0.515 μm. Our curve given in Fig. 18 indicates that the calculated position is within this range for the one-third normal aerosol model and either A = 0 or 0.15. It is unfortunate that the measurements could not have been extended to include the case of the sun nearer the horizon, as the calculations predict that

the position of the maximum moves toward the sun as Θ_0 decreases and is approximately 80° from the sun when $\Theta_0 = 0°$.

The angle χ which the direction of polarization (maximum intensity component) makes with the direction of the meridian plane containing the final photon direction is given by

$$\tan 2\chi = U/Q, \tag{2}$$

where U and Q are two of the four components of the Stokes vector (I, Q, U, V). The range $0° \leq \chi \leq 180°$ has been chosen for the principal value of χ. The angle χ is chosen in the range $0° \leq \chi \leq 90°$ when $U \geq 0$ and in the range $90° \leq \chi \leq 180°$ when $U \leq 0$. U is always negative for Rayleigh scattering, but may have either sign for aerosol scattering. U changes sign at the angles at which M^- (the element of the phase matrix in the first row and second column) is zero. The values of 0° and 180° for χ have equivalent physical meanings. For example, if χ is increasing as the zenith angle increases and reaches the value 180°, the curve immediately reappears at the bottom of the graph at 0°. This is not a real discontinuity in the motion of the direction of polarization, which rotates in a perfectly continuous manner; only the graphical representation has this jump.

The angle χ is given in Fig. 20 for $\Theta_0 = 40.88°$ and 80.18 and $\phi = 60°$ and 120°. There is no appreciable difference in the curves for the normal and one-third normal aerosol models nor is there an appreciable variation with surface albedo. Curves for both the transmitted and reflected radiation are shown in the figure and the values are nearly identical in both cases for corresponding angles. Clearly the Rayleigh scattering dominates the determination of χ and there are no discontinuities or rapid variations of χ as are found for scattering from a pure haze L layer (see II, Fig. 3). One of the reasons that changes in χ with amount of aerosols and surface albedo are so small in general is that χ is computed from the ratio of U to Q. It is found that even though the magnitude of U and Q can change drastically, their ratio changes very little.

V. Ellipticity

If a and b are proportional to the major and minor axes respectively of the ellipse described by the end point of the electric vector of the radiation, then the ellipticity (E) is defined as the ratio b/a. In terms of the four Stokes compoments I, Q, U, V the ellipticity is

$$E = - \tan \{ \tfrac{1}{2} \sin^{-1} [V(Q^2 + U^2 + V^2)^{-\frac{1}{2}}] \}. \qquad (3)$$

When the ellipticity is small, this reduces to

$$E \cong - \tfrac{1}{2} V(Q^2 + U^2 + V^2)^{-\frac{1}{2}} . \qquad (4)$$

It was shown in II that the simple relation

$$E \cong -V/2PI \qquad (5)$$

holds when the ellipticity is small. This equation reminds us that the ellipticity is zero whenver V is zero (which is always the case for Rayleigh scattering). The quantity V is also zero for any spherical polydispersion in the principal plane. The polarization in general tends to be large in a region where the ellipticity is small. The above equations show that the ellipticity is small when PI>>V.

The incident solar radiation is unpolarized to a high approximation. If there were only Rayleigh scattering in the atmosphere, there could be no elliptically polarized light. The ellipticity arises from multiple scattering from the aerosol component. Incident unpolarized radiation cannot create a circular component from a single scattering, since the phase matrix for spherical particles has a zero entry in the fourth row and first column. The photon must be scattered several times to be elliptically polarized. The ellipticity of radiation scattered from a pure haze L layer is studied in II. As in that article, all graphs in this article show the absolute value of the ellipticity.

The ellipticity for three solar zenith angles (Θ_0 = 21.20°, 40.88°, 60.53°) is given is Fig. 21 in the plane ϕ = 30° and 150° for the transmitted photons and a normal aerosol amount. These curves may be compared with Fig. 7 of II which gives the ellipticity for a pure haze L layer for Θ_0 = 31.43° (a value intermediate between the first two values of Θ_0 given in Fig. 20). If the comparison is made for the haze L curve with τ = 0.25, it is seen that the real atmosphere model results differ only in detail from the pure haze L layer. The position of the zeros of the curves is changed somewhat by the Rayleigh scattering of the real atmosphere model.

The ellipticity for Θ_0 = 80.18°, the plane ϕ = 30° and 150°, and the one-third normal and normal aerosol models is given in Fig. 22 for the transmitted radiation. All the ellipticity graphs in this article are for a surface albedo A = 0, since the variation with surface albedo could hardly be shown in the scale of these figures; the typical variation between the values for A = 0 and 0.9 is a few percent. The ellipticity, of course, decreases in general as the aerosol amount decreases. As the aerosol amount decreases to smaller values than shown here, the ellipticity decreases in direct proportion to the aerosol amount (see discussion in II) and this is even approximately true at many angles when the one-third normal and normal aerosol curves are compared in Fig. 22. It is interesting to compare Fig. 22 with Fig. 10 of II. The curve for τ = 0.25 in the latter figure has the same number of zeros as the one for the real atmosphere model, but their position in some cases is considerably displaced.

The ellipticity for the reflected photons for three solar zenith angles (21.20°; 40.88°; 60.53°) in the plane ϕ = 30° and 150° is shown in Fig. 23. The position of the zero points is not changed appreciably from a pure haze L layer (compare Fig. 6 of II). The main new feature is the relatively large values for the ellipticity (as large as 0.04) in the ϕ = 150° plane for the real atmosphere for Θ_0 = 21.20° and 40.88°.

The ellipticity for the reflected photons for $\Theta_0 = 80.18°$ and $\phi = 30°$ and 150° is given in Fig. 24 for both the one-third normal and the normal aerosol models. In this case the variation of the ellipticity is quite different from that for a pure haze L layer (see Fig. 9 of II). Unfortunately since the ellipticity only develops through the multiple scattering of the photons, there is no simple physical explanation for curves such as these. Again at many angles the ellipticity is approximately proportional to the aerosol amount.

VI. Conclusions

The radiance, amount and direction of polarization, and ellipticity of the solar radiation which has undergone multiple scattering in a model earth's atmosphere has been calculated. The variation of these quantities with solar zenith angle, aerosol amount, and surface albedo was investigated. A comparison of the calculated values with such experimental measurements as are available shows general qualitative agreement, even though the experimental conditions are never the same as those assumed for the model.

A measurement of the position of the neutral points in the principal plane should be a sensitive means of determining the characteristics of the aerosol particles in the atmosphere. The position of the neutral points is insensitive to the surface albedo, typically varying only a few degrees, as the albedo changes from zero to 0.9. The angular distance of the neutral points from the sun is also relatively insensitive to the solar zenith angle. It is, however, sensitive to the number of aerosol particles in the atmosphere and especially to the characteristics of their single scattering polarization curve, particularly for scattering angles around 20° (for transmitted photons) and around 160° (for reflected photons). The single scattering polarization changes greatly in character as the index of refraction and the size distribution of the aerosols is varied. Thus, changes in these two quantities for

the arosols in the real atmosphere should cause measurable variations in the neutral point positions. The positions of the Arago point is especially sensitive to the sign of the single scattered polarization for scattering angles around 180°.

The value of the maximum polarization in the principal plane containing the solar direction depends on the aerosol amount, the surface albedo, and the solar zenith angle. There exists a range of solar zenith angles for the reflected radiation where the position of the maximum polarization value is especially sensitive to the aerosol amount, e. g. when A = 0.15, this occurs for solar zenith angles between about 35° and 50°. This suggests another possible method for obtaining information about the aerosols in the atmosphere.

The ellipticity curves for the real atmosphere are qualitatively similar to those obtained for scattering from pure aerosol layers. They are little modified by the Rayleigh scattering which occurs in the real atmosphere. Since each kind and size distribution of aerosols has a characteristic ellipticity curve, a measurement of this quantity in the real atmosphere should provide considerable information about the nature of the aerosols that are present.

References

1. G. W. Kattawar, G. N. Plass and S. J. Hitzfelder, Appl. Opt. 15, xxx (1976).
2. G. N. Plass, G. W. Kattawar and S. J. Hitzfelder, Appl. Opt. 15, xxx (1976).
3. G. N. Plass and G. W. Kattawar, Appl. Opt. 9, 1122 (1970).
4. M. Tanaka, J. Meteorol. Soc. Japan, 49, 296, 321, 333 (1971).
5. Z. Sekera, Adv. Geophys. 3, 43 (1956).
6. L. Elterman, R. Wexler and D. T. Chang, Appl. Opt. 8, 893 (1969); also Air Force Cambridge Research Laboratories Report 68-0153 (1968).
7. D. Deirmendjian, Electromagnetic Scattering on Spherical Polydispersions (American Elsevier, New York, 1969).
8. G. W. Kattawar and G. N. Plass, Appl. Opt. 6, 1377 (1967).
9. G. W. Kattawar, S. J. Hitzfelder and J. Binstock, J. Atmos. Sci. 30, 289 (1973).
10. G. N. Plass, G. W. Kattawar and F. E. Catchings, Appl. Opt. 12, 314, 1071 (1973).
11. S. Chandrasekhar, Radiative Transfer (Oxford Univ. Press, New York, 1950).
12. K. L. Coulson, J. V. Dave and Z. Sekera, Tables Related to Radiation Emerging from a Planetary Atmosphere with Rayleigh Scattering (University of California Press, Los Angeles, 1960).
13. K. L. Coulson, J. Quant. Spectrosc. Radiat. Transfer 11, 739 (1971).
14. Z. Sekera et al., Investigation of the Polarization of Skylight, Final Rept. AF 19(122)-239, University of California, Los Angeles (1955).

Table I. Angular Distance Between Neutral Points and Sun or Antisun

Normal Aerosol Amount

		Brewster			Babinet		
	Θ_o	A = 0	0.15	0.90	A = 0	0.15	0.90
Reflected	0°	20.4°	20.3°	19.3°	20.4°	20.3°	19.3°
	21.20°	22.2°	22.0°	19.4°	19.3°	19.3°	19.3°
	40.88°	23.5°	23.0°	19.8°	22.0°	21.9°	21.4°
	60.53°	23.2°	22.8°	20.4°	22.6°	22.4°	21.4°
	80.18°	10.2°*	10.0°*	10.3°*	22.3°	22.2°	21.8°
Transmitted	0°	---	---	---	---	---	---
	21.20°	4.4°	4.1°	---	2.8°	2.6°	---
	40.88°	7.6°	7.2°	4.0°	6.8°	6.5°	4.2°
	60.53°	10.5°	10.2°	8.6°	9.3°	9.1°	7.8°
	80.18°	26.0°*	25.9°*	25.4°*	11.6°	11.6°	11.0°

One-Third Normal Aerosol Amount

Reflected	0°	---	---	---	---	---	---
	21.20°	10.7°	10.3°	8.3°	7.4°	7.2°	6.5°
	40.88°	15.4°	14.9°	11.5°	12.8°	12.6°	11.5°
	60.53°	18.6°	18.1°	16.0°	16.3°	16.2°	15.0°
	80.18°	14.2°*	14.1°*	13.1°	18.7°	18.7°	18.1°
Transmitted	0°	---	---	---	---	---	---
	21.20°	5.0°	4.7°	3.1°	3.5°	3.4°	2.2°
	40.88°	8.8°	8.4°	6.6°	7.6°	7.5°	6.4°
	60.53°	12.3°	12.0°	10.5°	10.3°	10.2°	9.3°
	80.18°	21.8°*	21.7°*	21.3°*	13.9°	13.8°	13.4°

* Arago point

Captions for Figures

Fig. 1 Diffuse transmitted radiance at the earth's surface for model atmospheres with normal and one-third normal aerosol amounts as a function of zenith angle of observation. The sun is at the zenith ($\theta_0 = 0^0$). Curves are given for three values of the surface albedo (A = 0, 0.15, 0.90) as well as for the photons that have undergone only a single scattering event. The incoming solar flux is normalized to unity in a direction perpendicular to the solar beam.

Fig. 2 Diffuse transmitted radiance for A = 0.15 and normal aerosol amount for five solar zenith angles ($\theta_0 = 0^0$, 21.20^0, 40.88^0, 60.53^0, 80.18^0) in the principal plane ($\phi = 0^0$ and 180^0). The antisolar horizon is at the right of the graph and the solar horizon at the left.

Fig. 3 Reflected radiance at the top of the atmosphere for model atmospheres with normal and one-third normal aerosol amounts as a function of nadir angle of observation. The sun is at the zenith ($\theta_0 = 0^0$). Curves are given for A = 0, 0.15 and 0.90 and for single scattered photons.

Fig. 4 Reflected radiance for $\theta_0 = 80.18^0$ in the principal plane ($\phi = 0^0$ and 180^0). The antisolar horizon is at the left of the graph and the solar horizon is at the right.

Fig. 5 Reflected randiance in the principal plane for normal aerosol model for $\theta_0 = 0^0$ and 80.18^0 with A = 0 and for $\theta_0 = 0^0$, 21.20^0, 40.88^0, 60.53^0, 80.15^0 with A = 0.15.

Fig. 6 Polarization of the transmitted photons in the principal plane for A = 0.15 and $\theta_0 = 0^0$, 21.20^0, 40.88^0, 60.53^0, 80.18^0 for normal aerosol model.

Fig. 7 Polarization of the transmitted photons with the sun at the zenith for the normal and one-third normal aerosol models and three values of the surface albedo.

Fig. 8 Polarization of the transmitted photons for $\Theta_0 = 80.18°$ in the principal plane ($\phi = 0°$ and $180°$). Curves are given for the normal and one-third normal aerosol models and three values of the surface albedo.

Fig. 9 Polarization of the transmitted photons for $\Theta_0 = 80.18°$ and $\phi = 60°$ and $120°$.

Fig. 10 Polarization of the transmitted photons for $\Theta_0 = 80.18°$ and $\phi = 90°$.

Fig. 11 Polarization of the reflected photons in the principal plane for A = 0.15 and $\Theta_0 = 0°$, $21.20°$, $40.88°$, $60.53°$, $80.18°$.

Fig. 12 Polarization of the reflected photons for $\Theta_0 = 0°$.

Fig. 13 Polarization of the reflected photons for $\Theta = 80.18°$ and $\phi = 0°$ and $180°$.

Fig. 14 Polarization of the reflected photons for $\Theta_0 = 40.88°$ and $\phi = 0°$ and $180°$. The curves for $\phi = 180°$ between nadir angles of $14°$ and $67°$ have been multiplied by 10 for clarity.

Fig. 15 Angle between Babinet neutral point and sun or antisun as a function of solar zenith angle. For comparison the curve is given for scattering from a pure Rayleigh layer of optical thickness 0.1 (appropriate for a wavelength of 0.55 μm).

Fig. 16 Angle between Brewster and Arago neutral points and sun or antisun as a function of solar zenith angle.

Fig. 17 Maximum polarization in principal plane as a function of solar zenith angle. Curves are given for three surface albedos (0.0, 0.15, 0.90), the one-third and normal aerosol models, as well as for single scattering from the normal aerosol model atmosphere.

Fig. 18 Zenith or nadir angle at which the maximum polarization is observed in principal plane as a function of the solar zenith angle.

Fig. 19 Maximum polarization in plane with $\phi = 90°$ as a function of solar zenith angle.

Fig. 20 Direction of polarization (χ) as a function of the zenith angle (for transmitted photons) or of nadir angle (for reflected photons). Curves are given for Θ_0 = 40.88° and 80.18°; ϕ = 60° and 120°; A = 0; normal aerosol model.

Fig. 21 Absolute value of ellipticity as a function of zenith angle for Θ_0 = 21.20°, 40.88°, 60.53°; ϕ = 30° and 150°; A = 0; normal aerosol model; for transmitted photons.

Fig. 22 Absolute value of ellipticity as a function of zenith angle for Θ_0 = 80.18°; ϕ = 30° and 150°; A = 0; one-third normal and normal aerosol models; for transmitted photons.

Fig. 23 Absolute value of ellipticity as a function of nadir angle for Θ_0 = 21.20°, 40.88°, 60.53°; ϕ = 30° and 150°; A = 0; normal aerosol model; for reflected photons.

Fig. 24 Absolute value of ellipticity as a function of nadir angle for Θ_0 = 80.18°; ϕ = 30° and 150°; A = 0; for reflected photons.

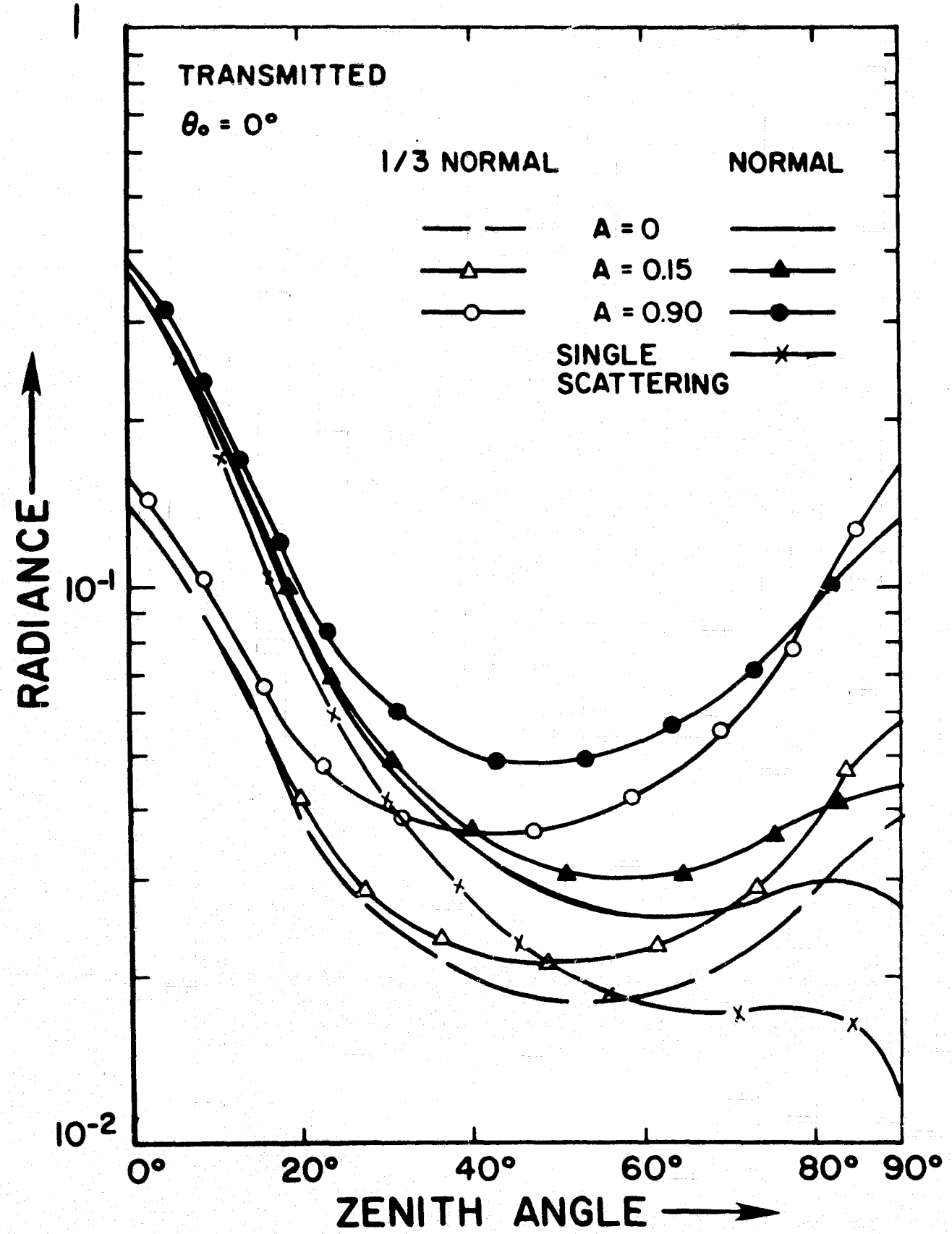
1
TRANSMITTED
θ_o = 0°
1/3 NORMAL
NORMAL
A = 0
A = 0.15
A = 0.90
SINGLE SCATTERING
RADIANCE
10^{-1}
10^{-2}
0°
20°
40°
60°
80°
90°
ZENITH ANGLE

Fig. 1

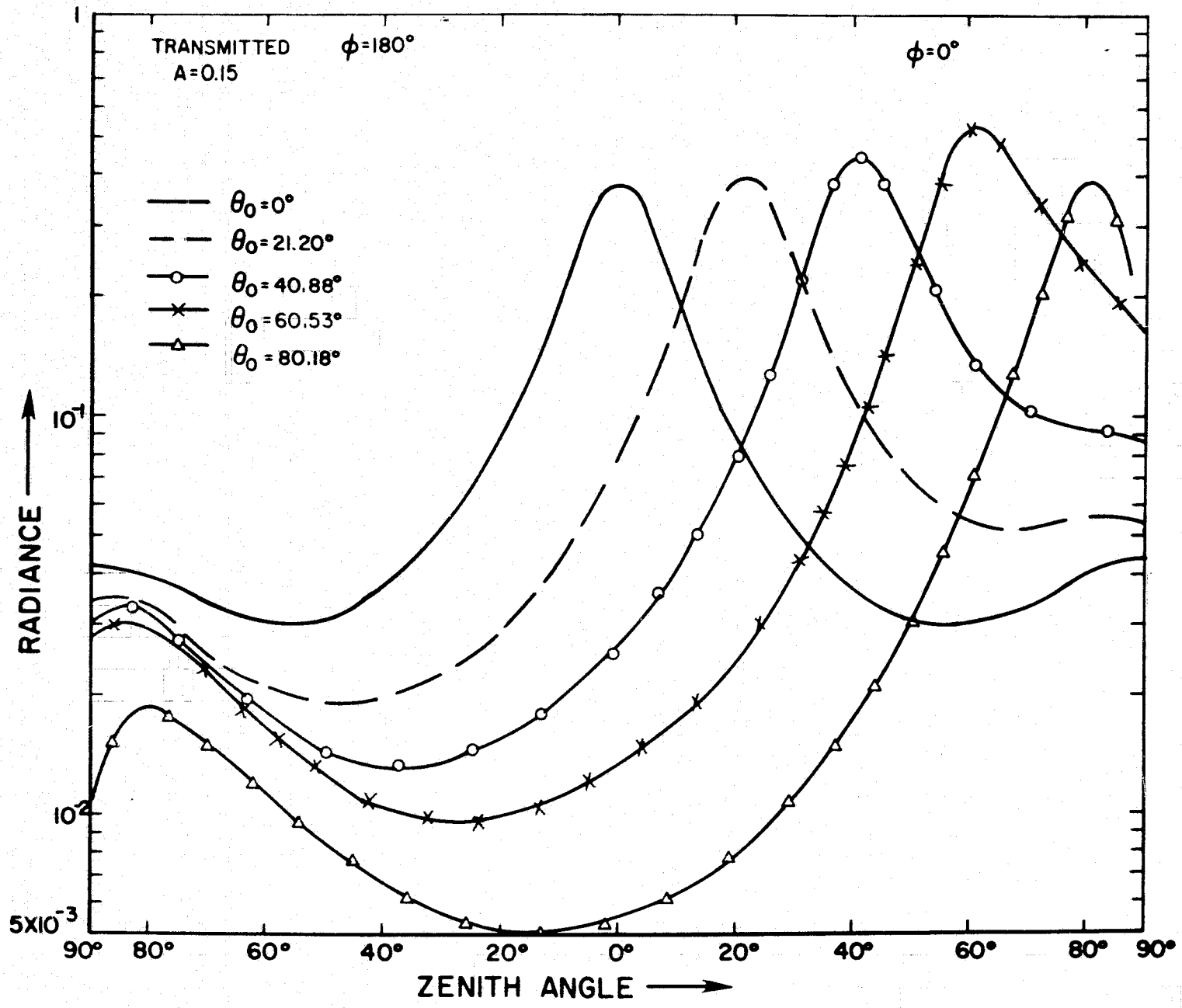
TRANSMITTED
A=0.15
ϕ=180°
ϕ=0°
θ_0=0°
θ_0=21.20°
θ_0=40.88°
θ_0=60.53°
θ_0=80.18°
1
10^{-1}
10^{-2}
$5X10^{-3}$
RADIANCE
90° 80° 60° 40° 20° 0° 20° 40° 60° 80° 90°
ZENITH ANGLE

Fig. 2

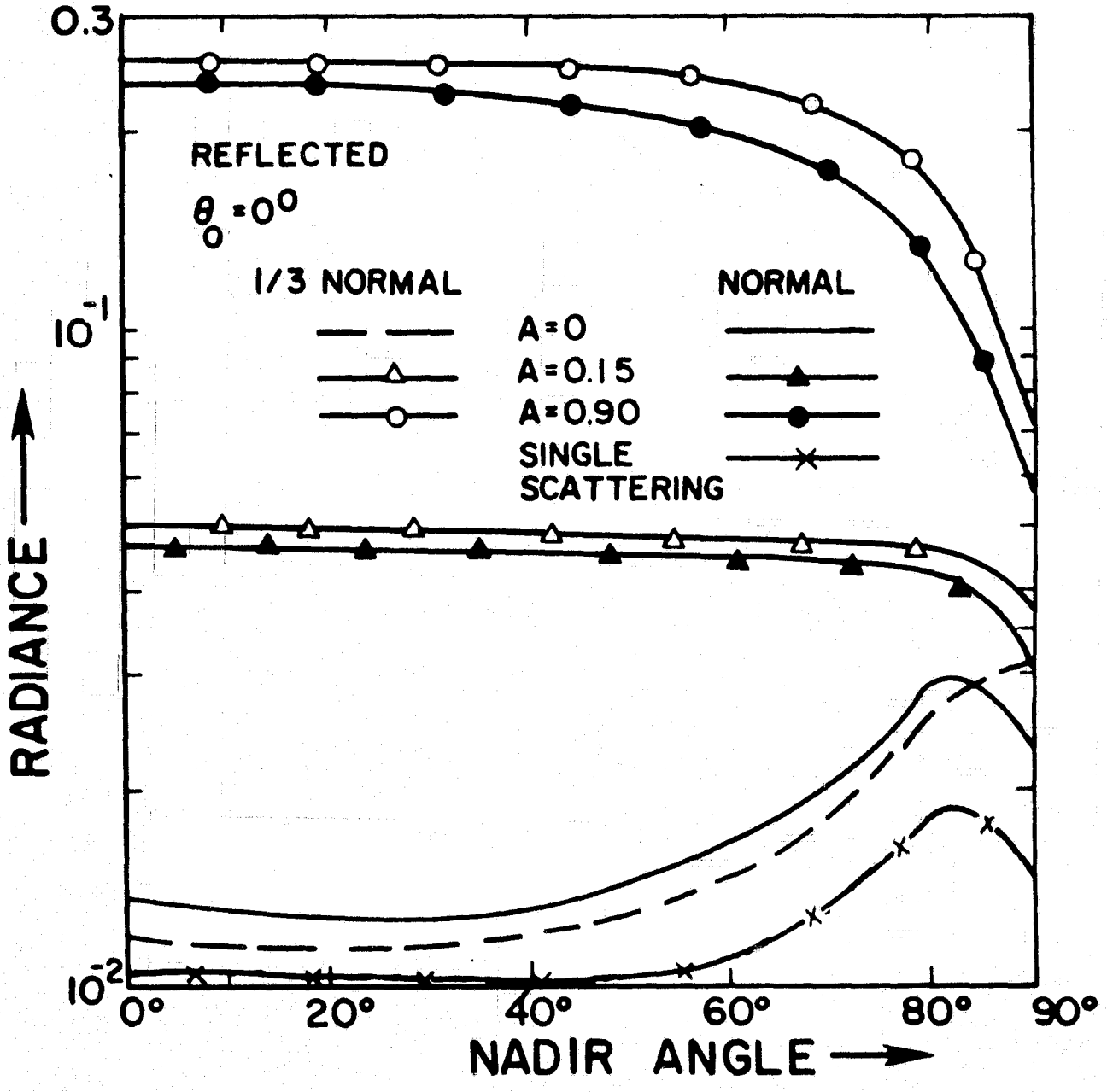
0.3
10^{-1}
10^{-2}
REFLECTED
$\theta_0 = 0^0$
1/3 NORMAL
NORMAL
A=0
A=0.15
A=0.90
SINGLE SCATTERING
RADIANCE
0°
20°
40°
60°
80°
90°
NADIR ANGLE

Fig. 3

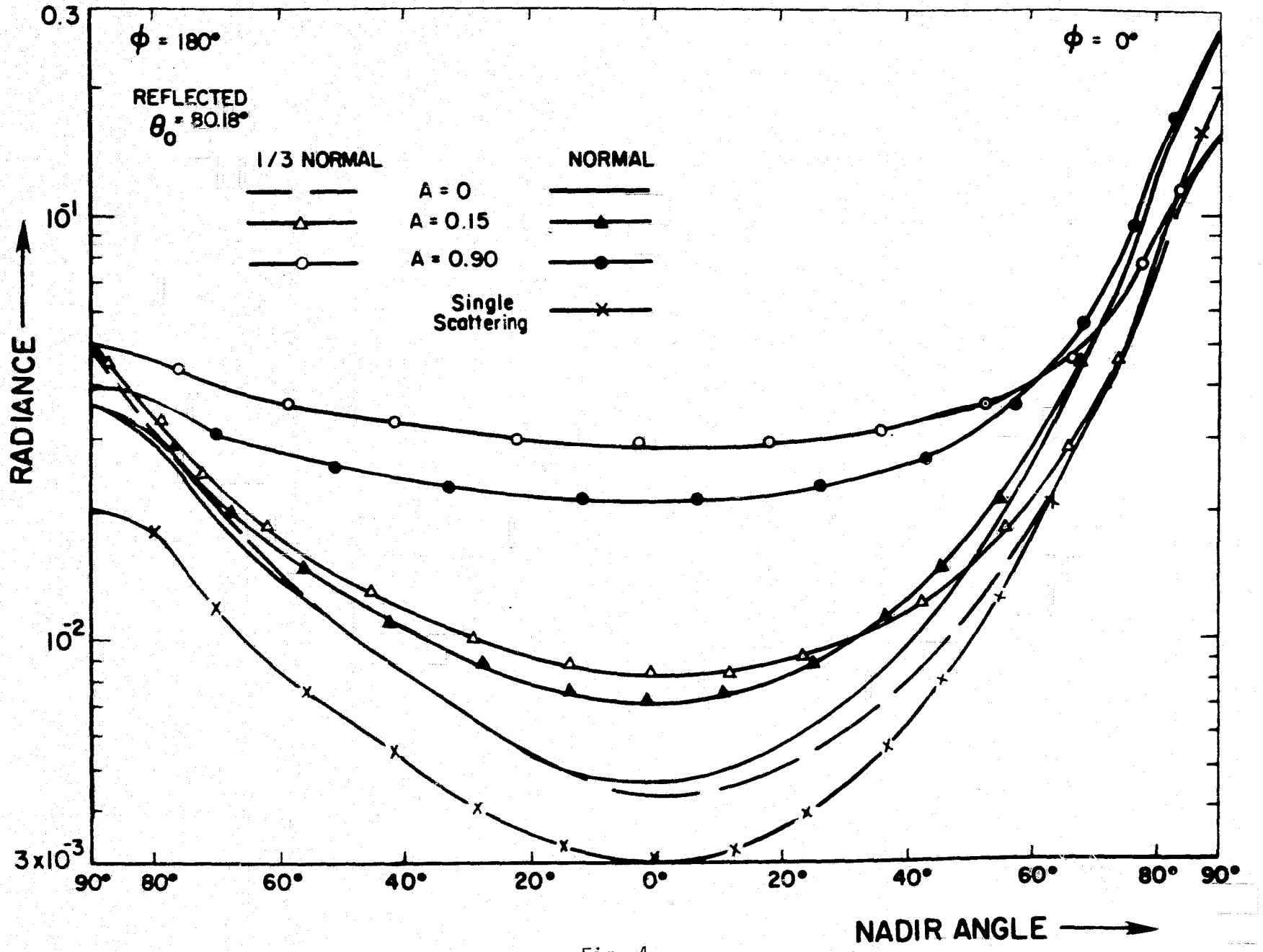
0.3
ϕ = 180°
ϕ = 0°
REFLECTED
θ_0 = 80.18°
1/3 NORMAL
NORMAL
A = 0
A = 0.15
A = 0.90
Single Scattering
10^{-1}
10^{-2}
3×10^{-3}
RADIANCE
90° 80° 60° 40° 20° 0° 20° 40° 60° 80° 90°
NADIR ANGLE

Fig. 4

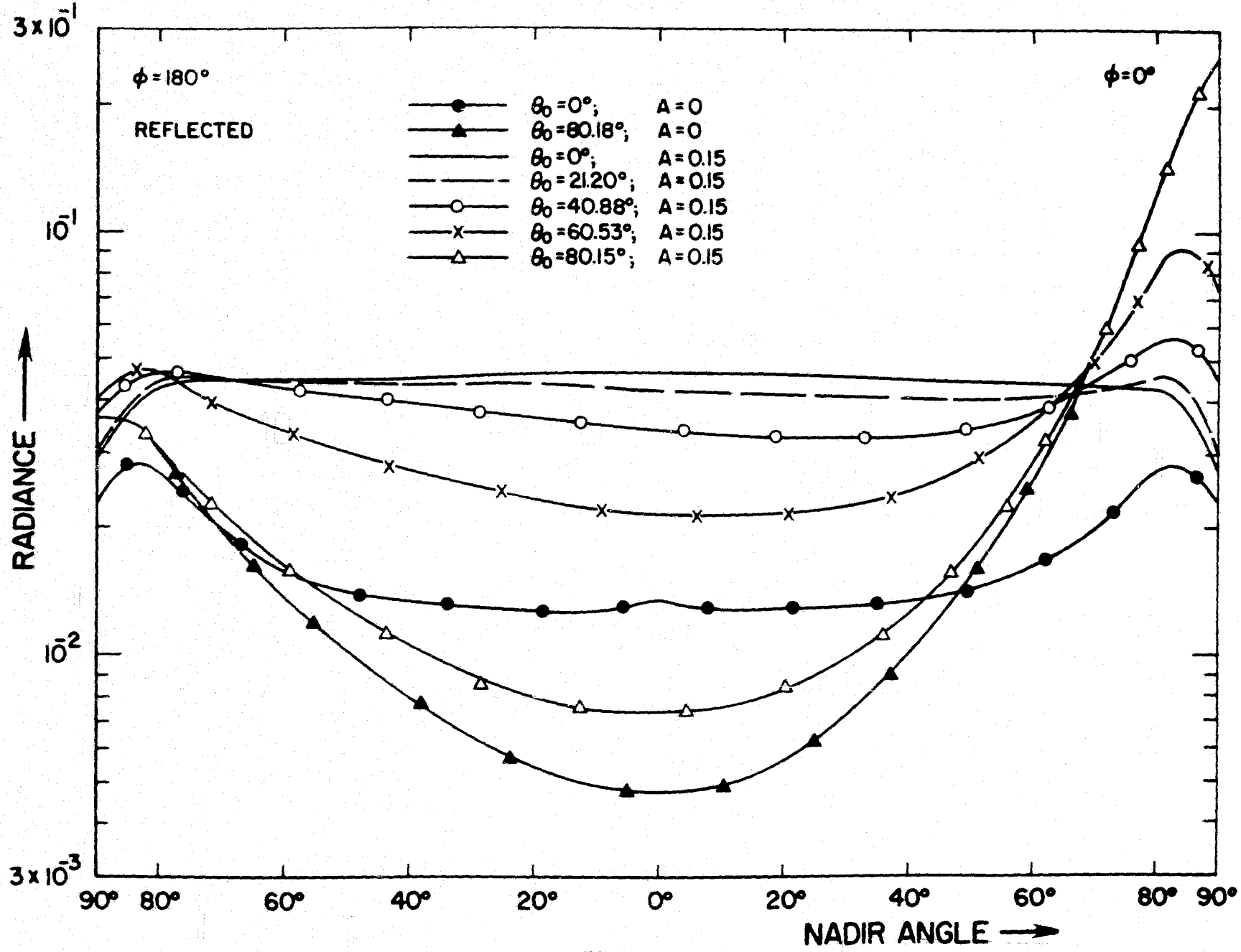
3x10⁻¹
10⁻¹
10⁻²
3x10⁻³
RADIANCE
φ=180°
REFLECTED
φ=0°
θ0=0°; A=0
θ0=80.18°; A=0
θ0=0°; A=0.15
θ0=21.20°; A=0.15
θ0=40.88°; A=0.15
θ0=60.53°; A=0.15
θ0=80.15°; A=0.15
90° 80° 60° 40° 20° 0° 20° 40° 60° 80° 90°
NADIR ANGLE

Fig. 5

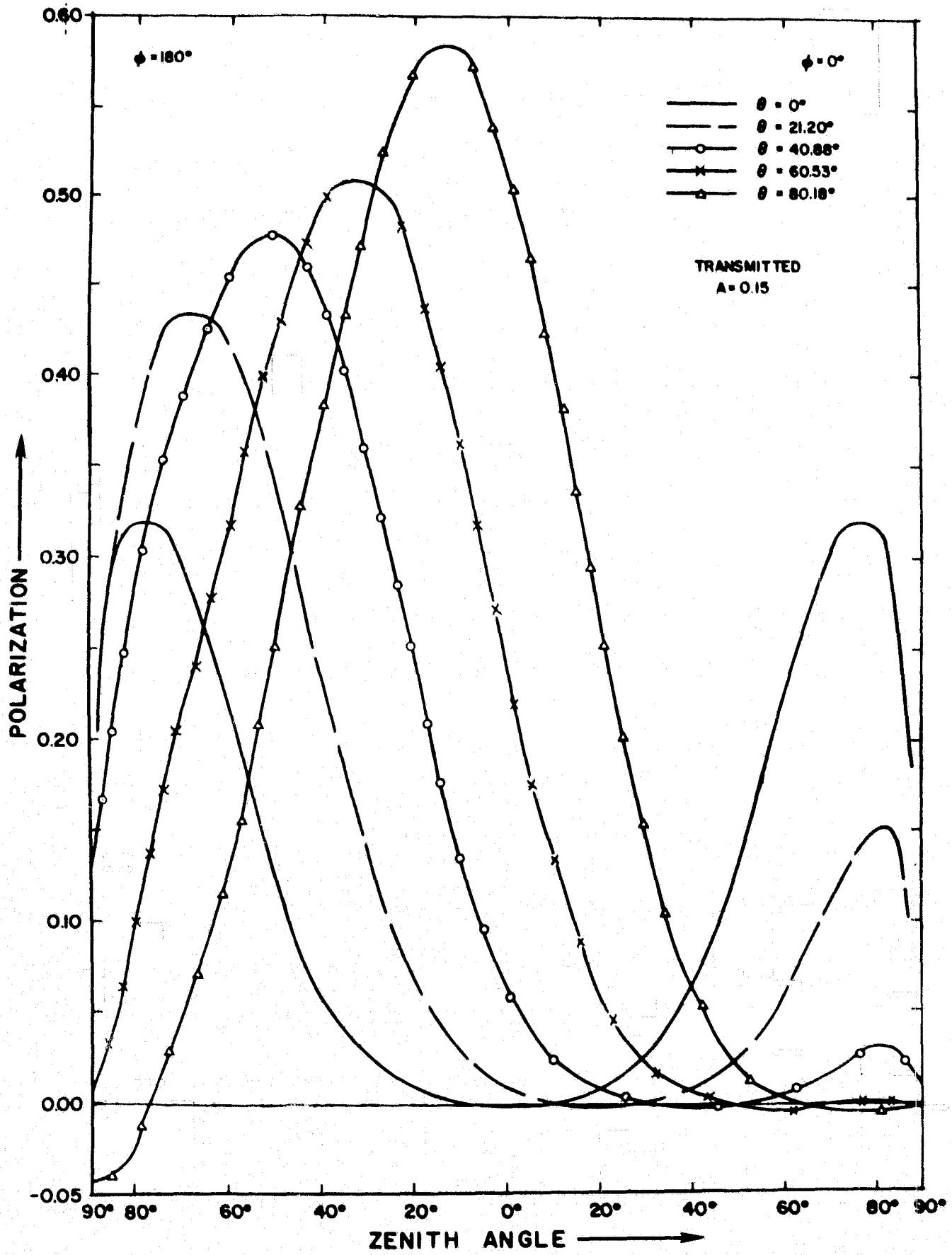
0.60
0.50
0.40
0.30
0.20
0.10
0.00
-0.05
POLARIZATION
φ = 180°
φ = 0°
θ = 0°
θ = 21.20°
θ = 40.88°
θ = 60.53°
θ = 80.18°
TRANSMITTED
A = 0.15
90° 80° 60° 40° 20° 0° 20° 40° 60° 80° 90°
ZENITH ANGLE

Fig. 6

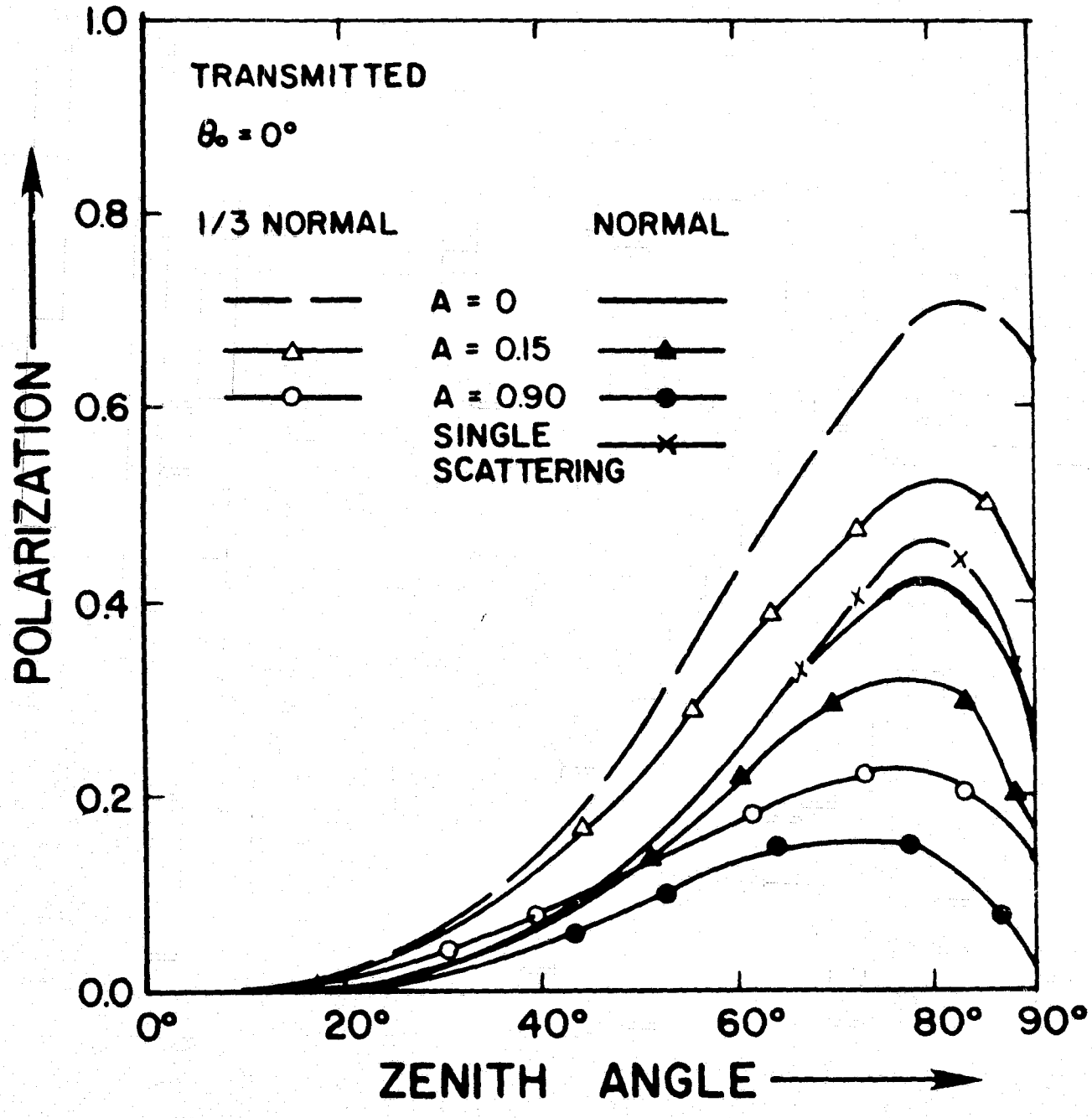
TRANSMITTED
$\theta_o = 0°$
1/3 NORMAL
NORMAL
A = 0
A = 0.15
A = 0.90
SINGLE SCATTERING
POLARIZATION
ZENITH ANGLE
1.0
0.8
0.6
0.4
0.2
0.0
0°
20°
40°
60°
80°
90°

Fig. 7

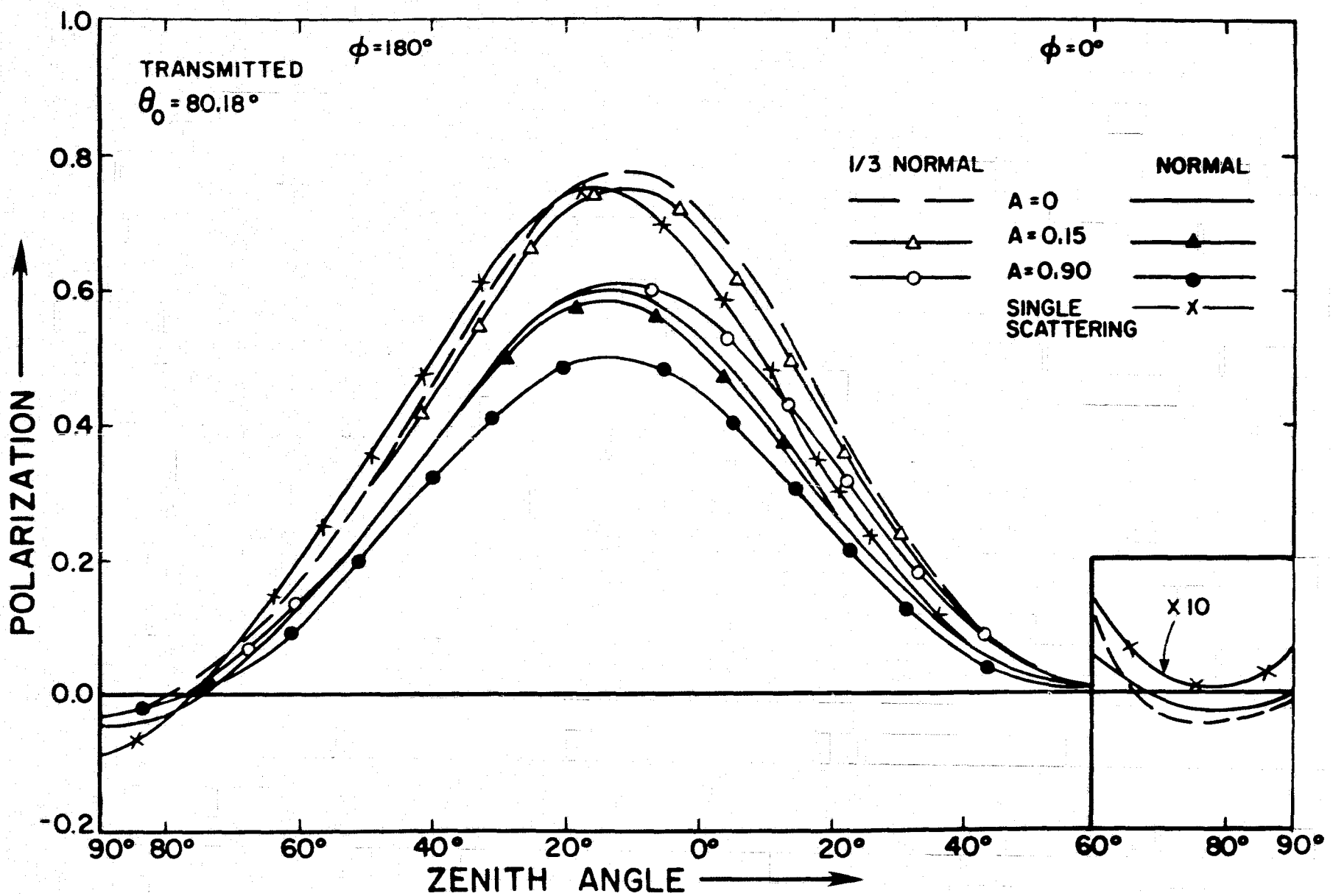
TRANSMITTED
$\theta_0 = 80.18°$
$\phi = 180°$
$\phi = 0°$
1/3 NORMAL
NORMAL
A = 0
A = 0.15
A = 0.90
SINGLE SCATTERING
X 10
POLARIZATION
ZENITH ANGLE
1.0
0.8
0.6
0.4
0.2
0.0
-0.2
90° 80° 60° 40° 20° 0° 20° 40° 60° 80° 90°

Fig. 8

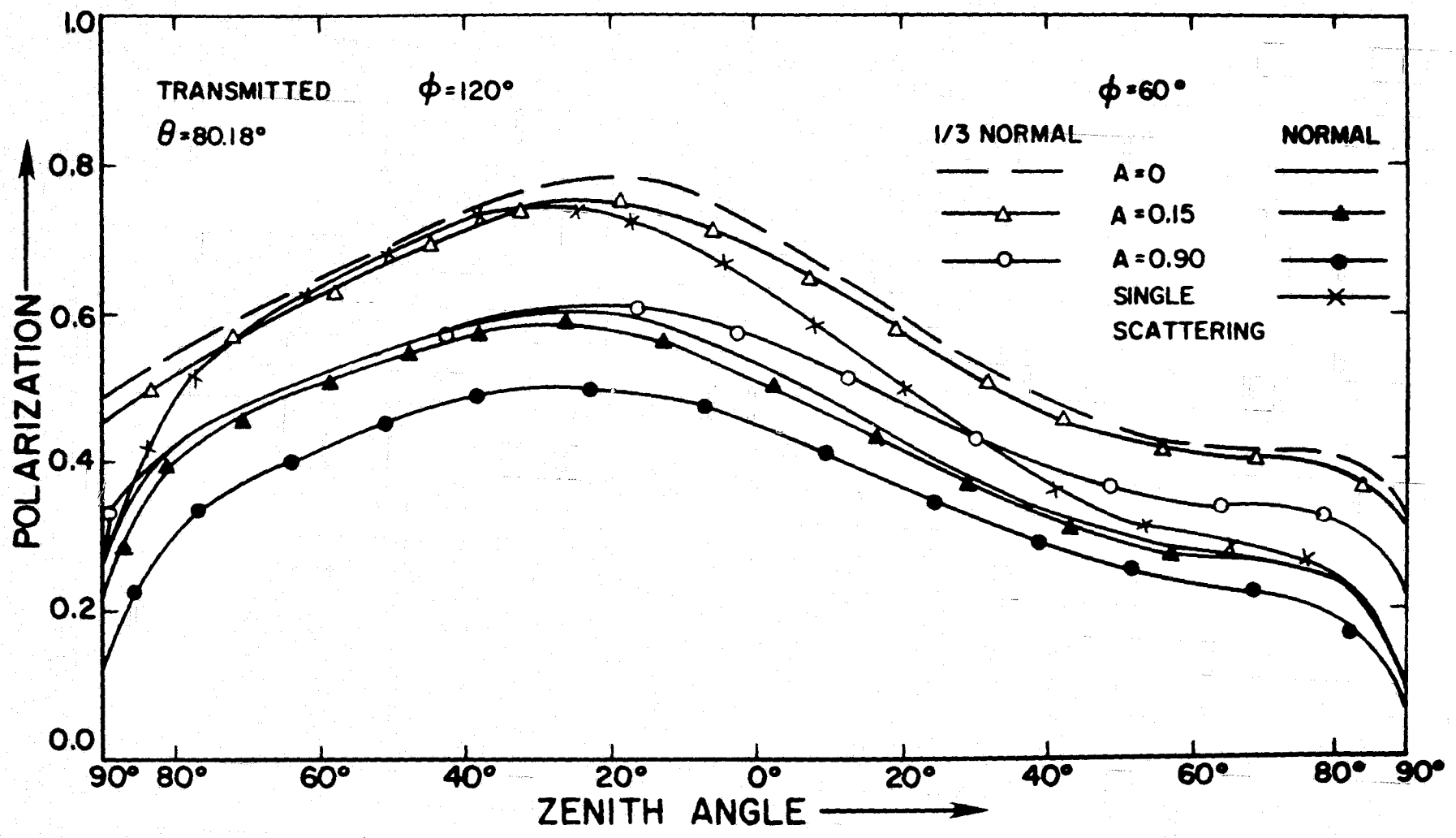
TRANSMITTED
θ=80.18°
φ=120°
φ=60°
1/3 NORMAL
NORMAL
A=0
A=0.15
A=0.90
SINGLE
SCATTERING
POLARIZATION
1.0
0.8
0.6
0.4
0.2
0.0
90° 80° 60° 40° 20° 0° 20° 40° 60° 80° 90°
ZENITH ANGLE

Fig. 9

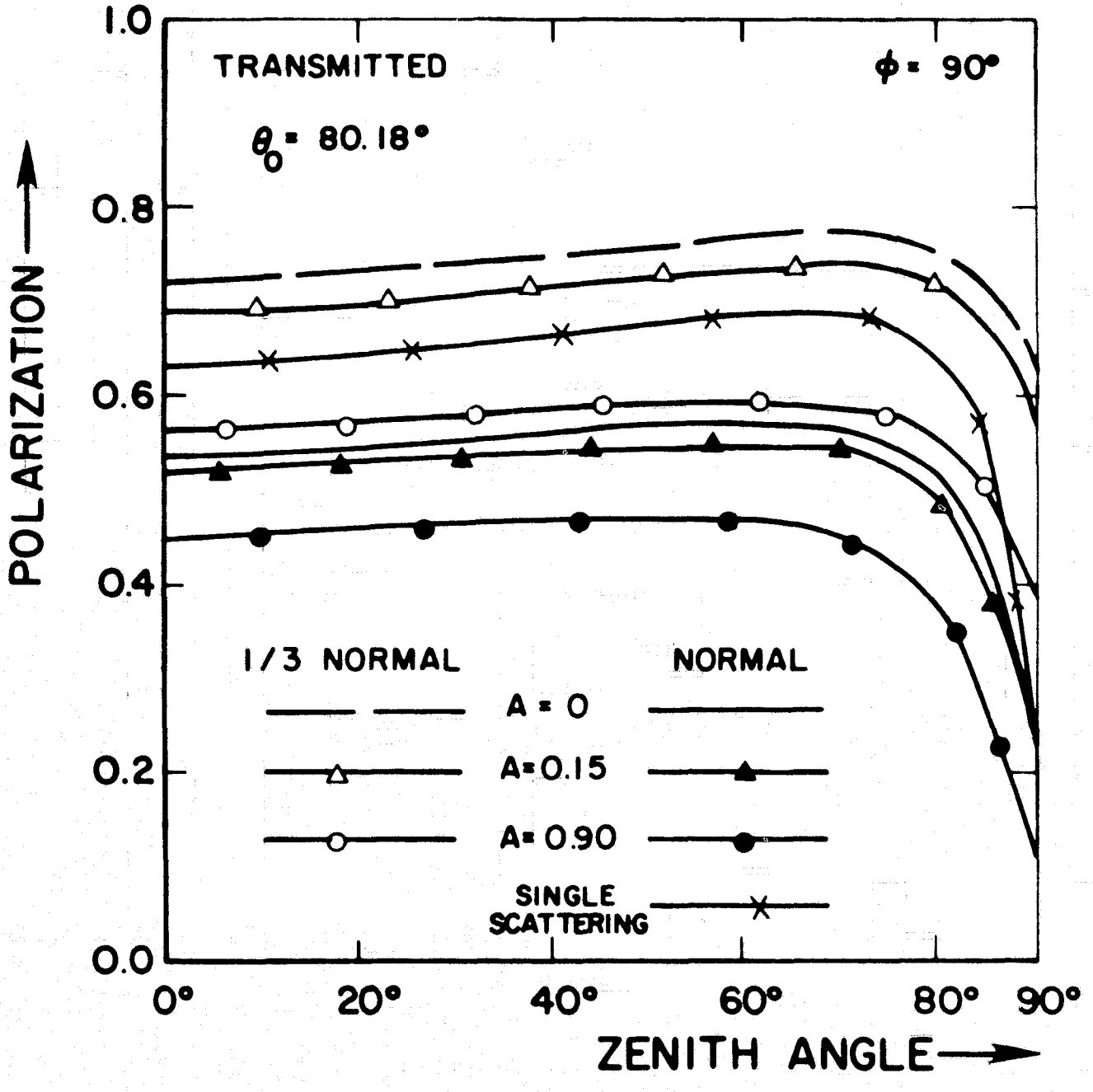
TRANSMITTED
ϕ = 90°
θ_0 = 80.18°
POLARIZATION
1.0
0.8
0.6
0.4
0.2
0.0
1/3 NORMAL
NORMAL
A = 0
A=0.15
A= 0.90
SINGLE SCATTERING
0°
20°
40°
60°
80°
90°
ZENITH ANGLE

Fig. 10

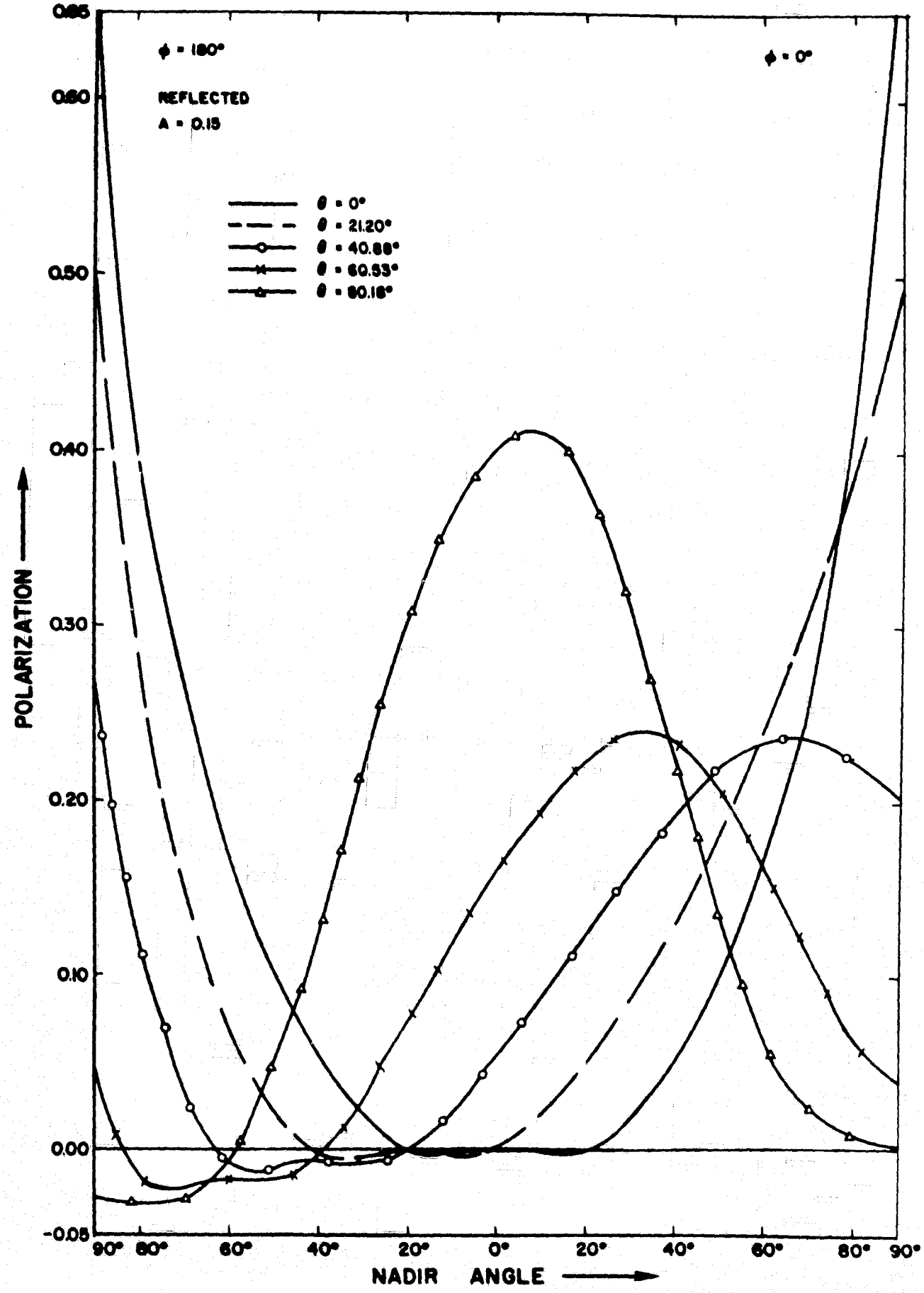
φ = 180°
φ = 0°
REFLECTED
A = 0.15
θ = 0°
θ = 21.20°
θ = 40.88°
θ = 60.53°
θ = 80.18°
0.65
0.60
0.50
0.40
0.30
0.20
0.10
0.00
-0.05
POLARIZATION
90° 80° 60° 40° 20° 0° 20° 40° 60° 80° 90°
NADIR ANGLE

Fig. 11

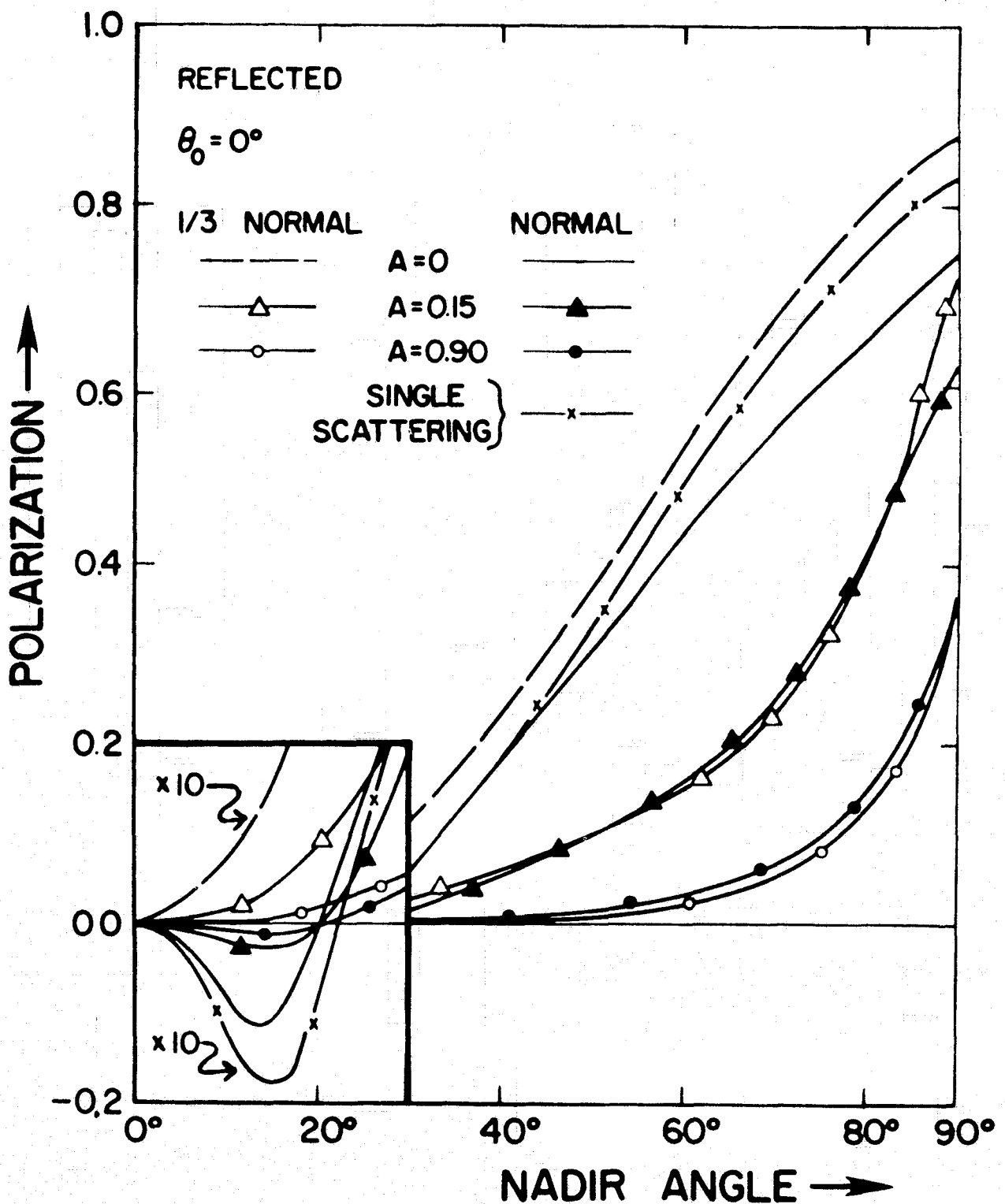
1.0
0.8
0.6
0.4
0.2
0.0
-0.2
POLARIZATION
REFLECTED
$\theta_0 = 0°$
1/3 NORMAL
NORMAL
A=0
A=0.15
A=0.90
SINGLE SCATTERING
x10
x10
0°
20°
40°
60°
80°
90°
NADIR ANGLE

Fig. 12

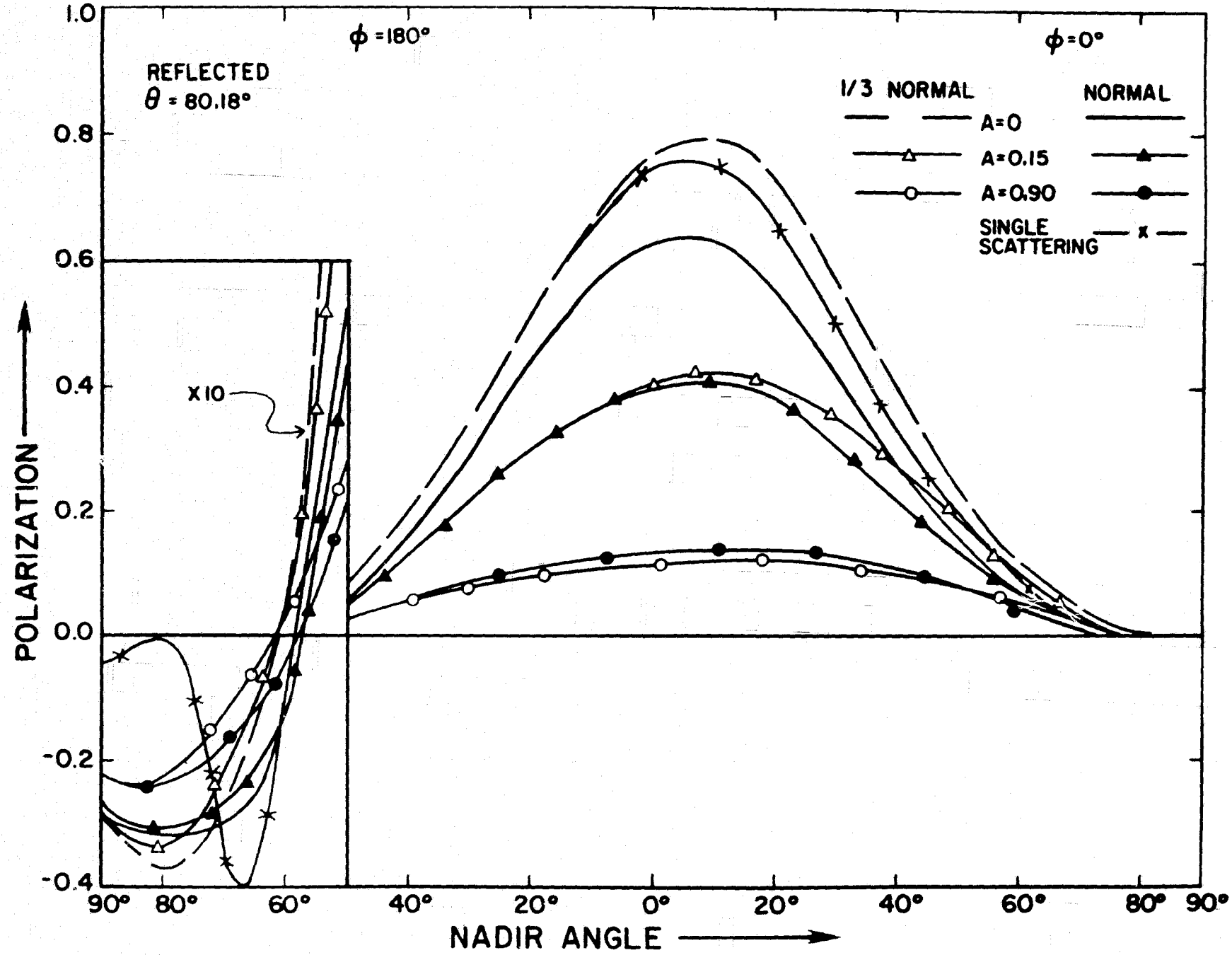
REFLECTED
θ = 80.18°
φ = 180°
φ = 0°
1/3 NORMAL
NORMAL
A=0
A=0.15
A=0.90
SINGLE SCATTERING
X10
POLARIZATION
NADIR ANGLE
1.0
0.8
0.6
0.4
0.2
0.0
-0.2
-0.4
90° 80° 60° 40° 20° 0° 20° 40° 60° 80° 90°

Fig. 13

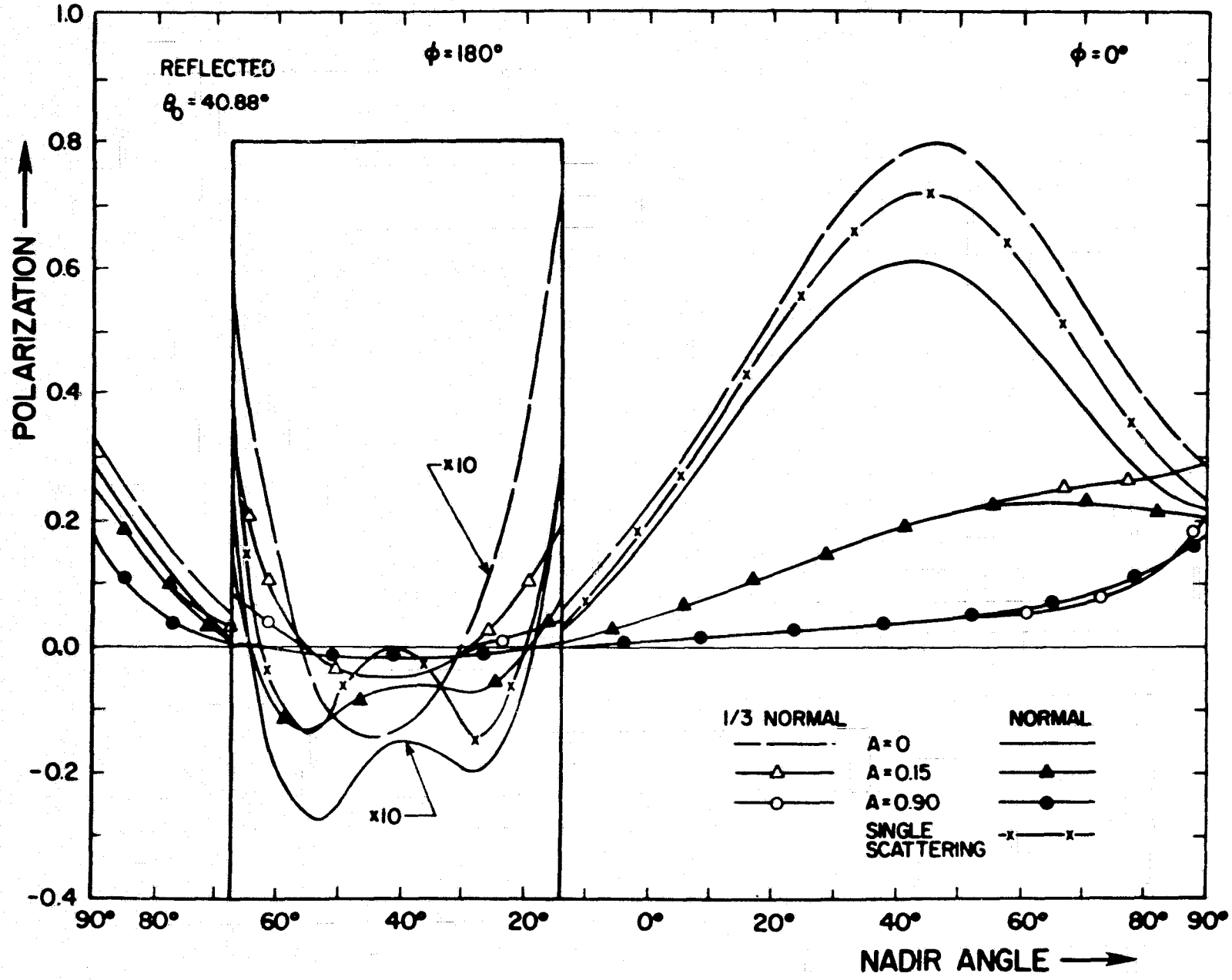
REFLECTED
$\theta_0 = 40.88°$
$\phi = 180°$
$\phi = 0°$
POLARIZATION
NADIR ANGLE
1.0
0.8
0.6
0.4
0.2
0.0
-0.2
-0.4
90° 80° 60° 40° 20° 0° 20° 40° 60° 80° 90°
x10
x10
1/3 NORMAL
NORMAL
A=0
A=0.15
A=0.90
SINGLE SCATTERING

Fig. 14

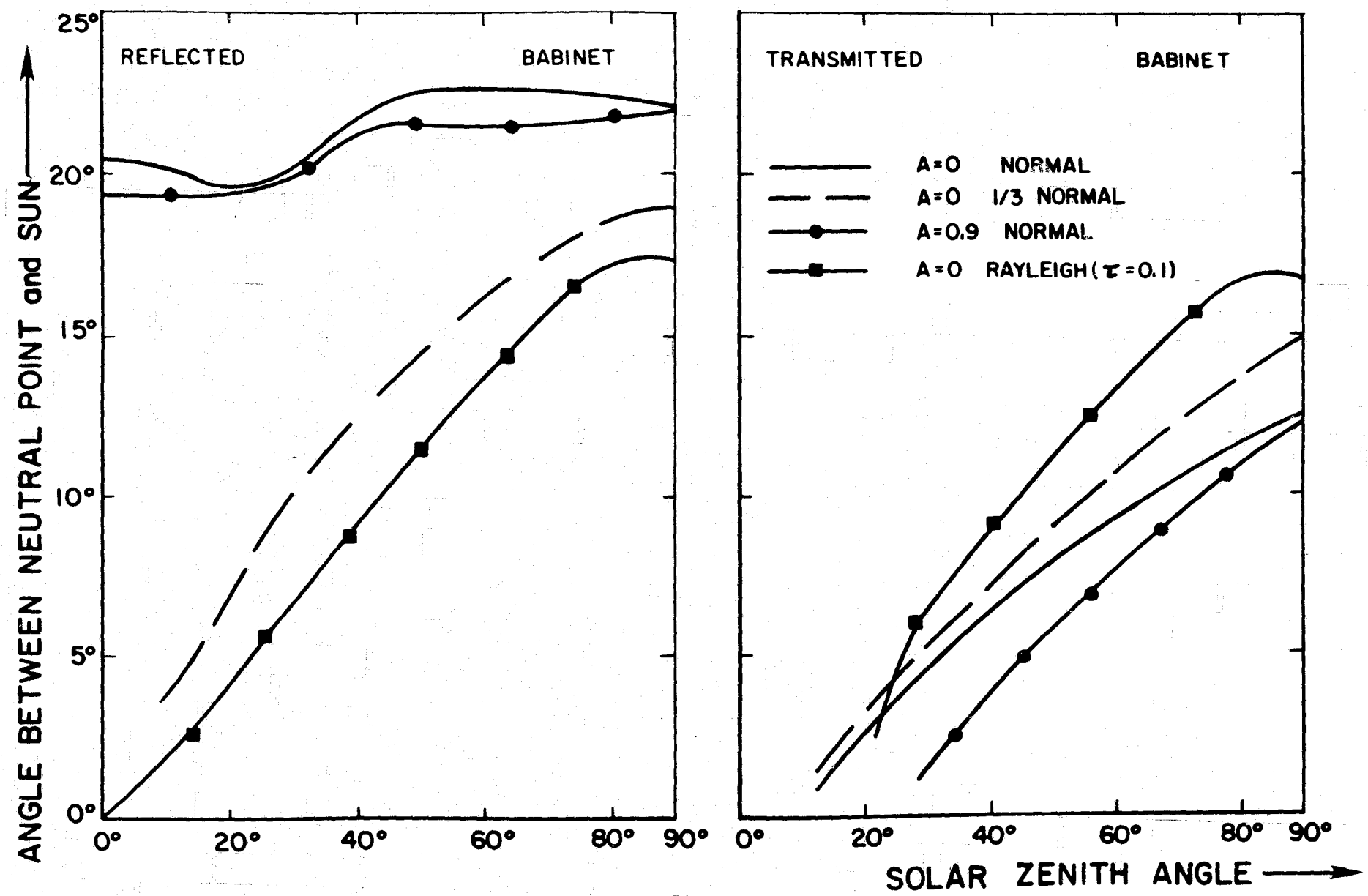
REFLECTED
BABINET
TRANSMITTED
BABINET
A=0 NORMAL
A=0 1/3 NORMAL
A=0.9 NORMAL
A=0 RAYLEIGH (τ=0.1)
ANGLE BETWEEN NEUTRAL POINT and SUN
SOLAR ZENITH ANGLE
0°
5°
10°
15°
20°
25°
0°
20°
40°
60°
80°
90°

Fig. 15

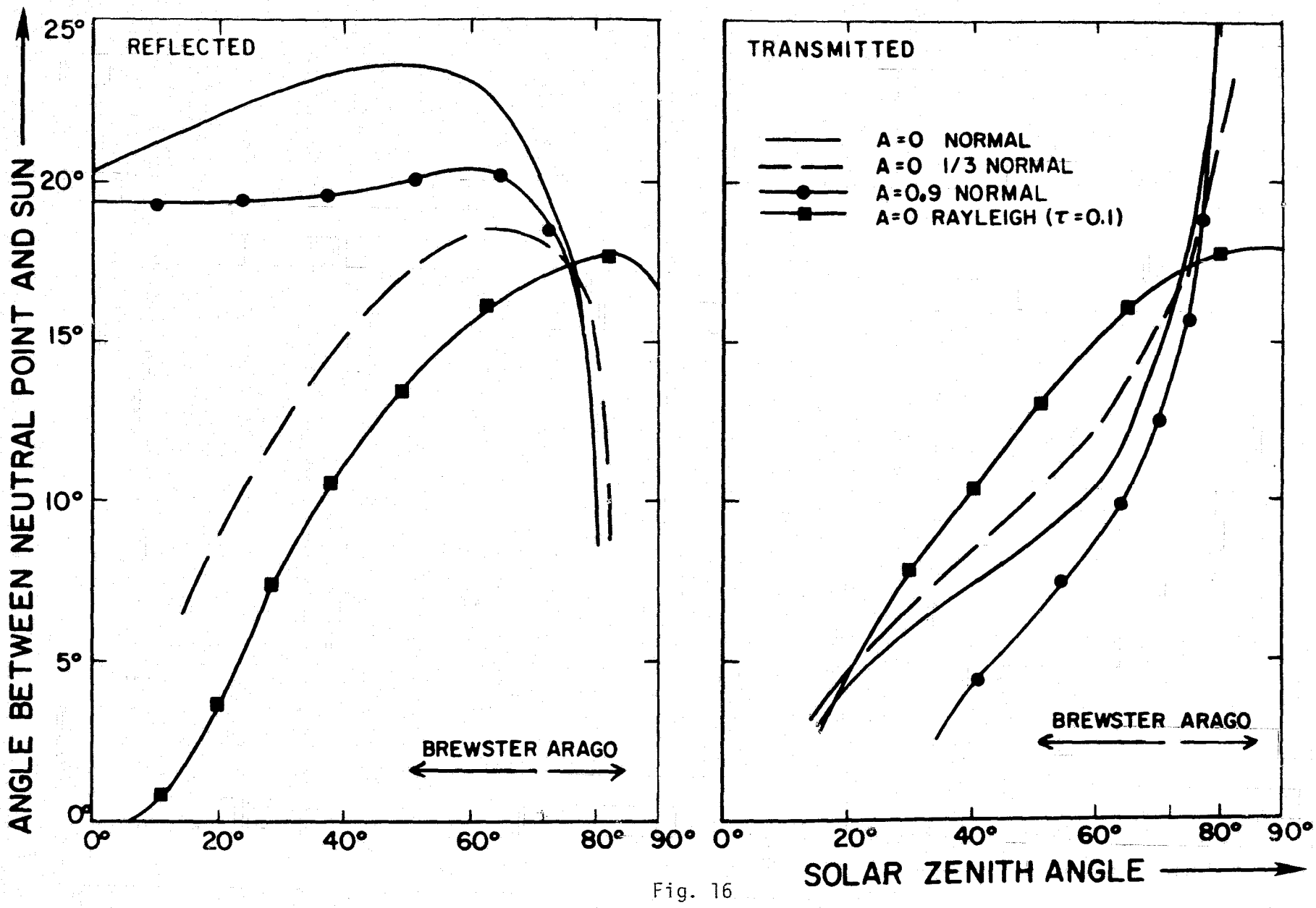
REFLECTED
TRANSMITTED
ANGLE BETWEEN NEUTRAL POINT AND SUN
SOLAR ZENITH ANGLE
A=0 NORMAL
A=0 1/3 NORMAL
A=0.9 NORMAL
A=0 RAYLEIGH (τ=0.1)
BREWSTER ARAGO
BREWSTER ARAGO
0°
5°
10°
15°
20°
25°
0°
20°
40°
60°
80°
90°
0°
20°
40°
60°
80°
90°

Fig. 16

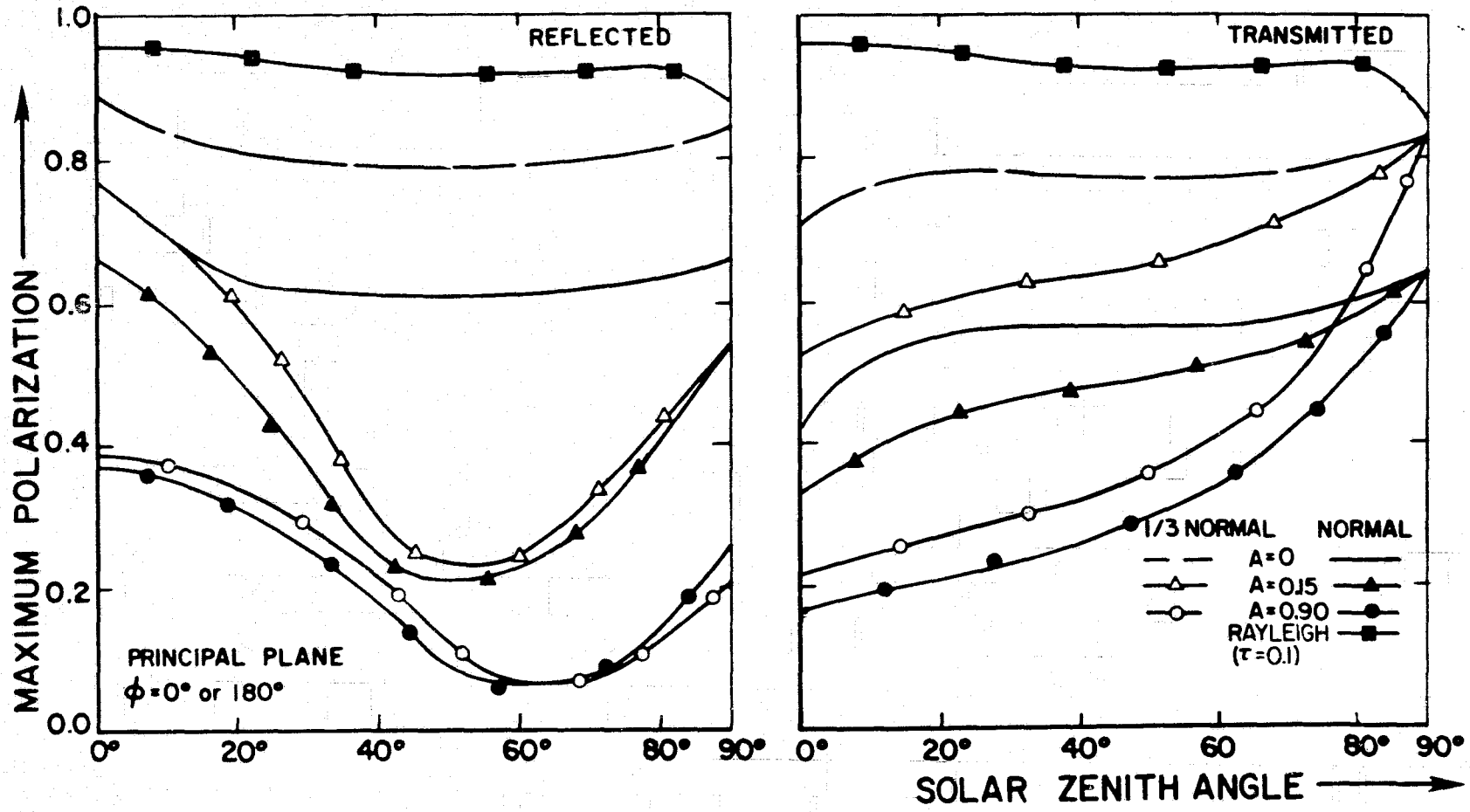
REFLECTED
TRANSMITTED
MAXIMUM POLARIZATION
1.0
0.8
0.6
0.4
0.2
0.0
PRINCIPAL PLANE
φ=0° or 180°
1/3 NORMAL
NORMAL
A=0
A=0.15
A=0.90
RAYLEIGH
(τ=0.1)
0°
20°
40°
60°
80°
90°
SOLAR ZENITH ANGLE

Fig. 17

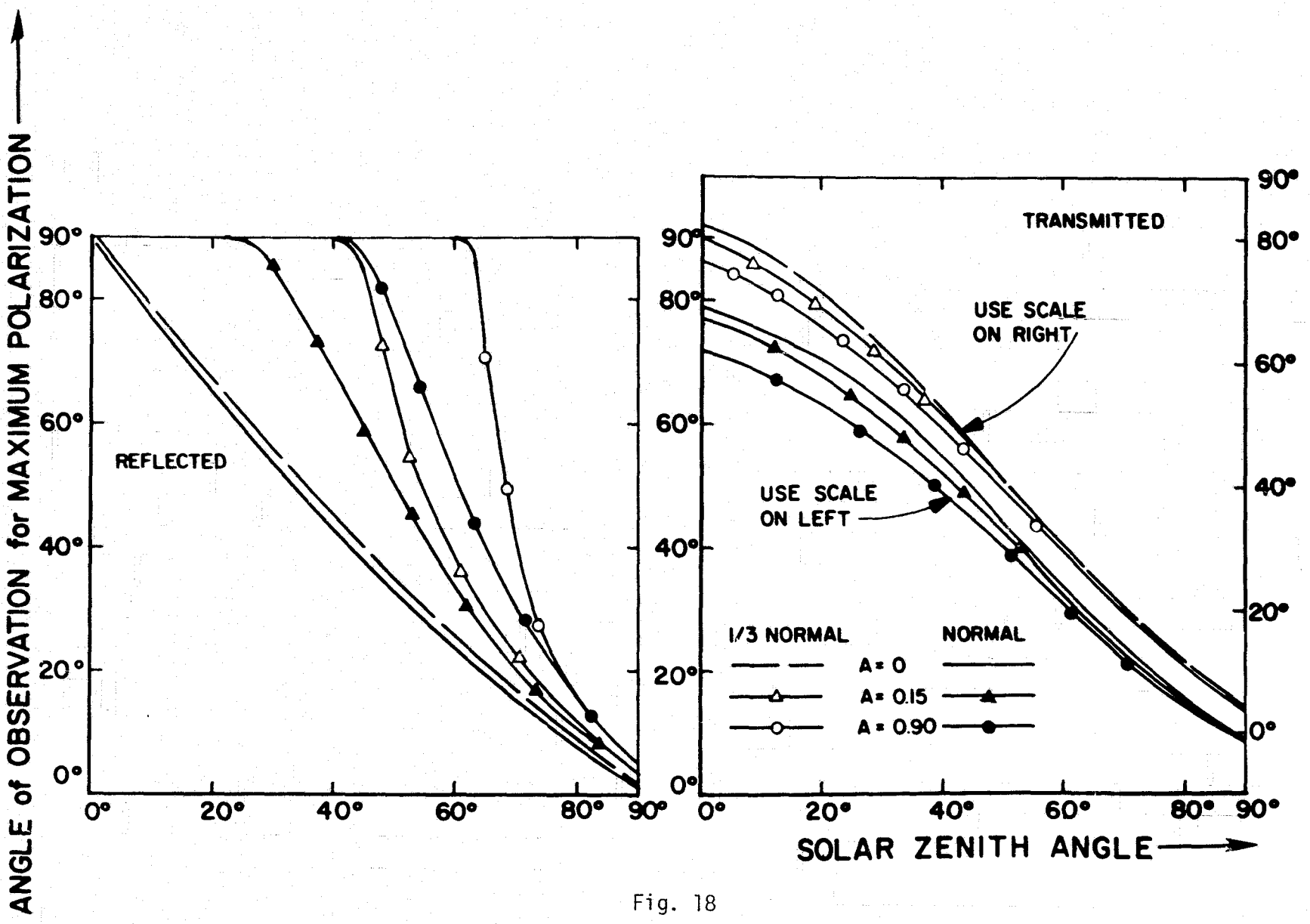
ANGLE of OBSERVATION for MAXIMUM POLARIZATION
REFLECTED
TRANSMITTED
USE SCALE ON RIGHT
USE SCALE ON LEFT
1/3 NORMAL
NORMAL
A = 0
A = 0.15
A = 0.90
0°
20°
40°
60°
80°
90°
SOLAR ZENITH ANGLE

Fig. 18

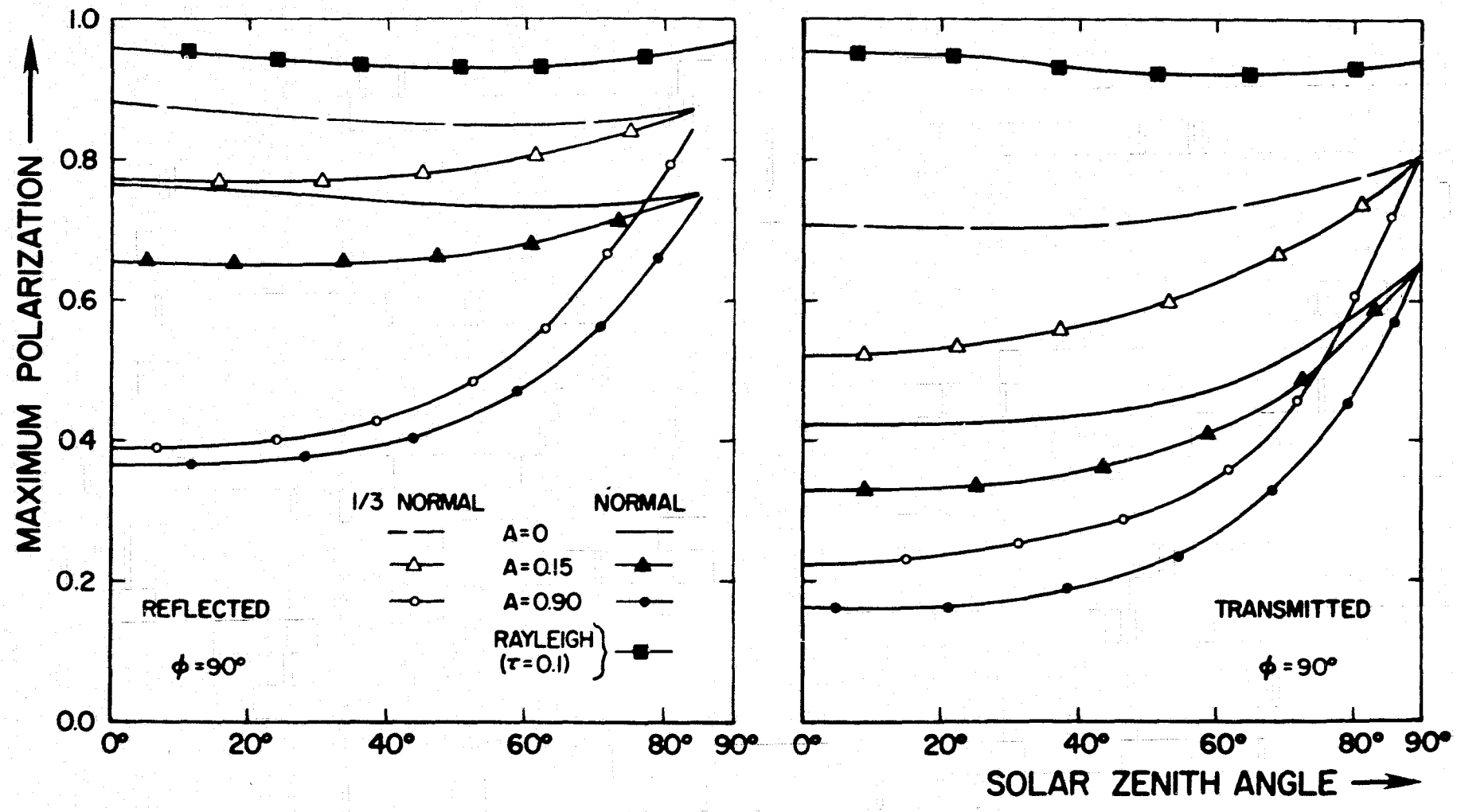
MAXIMUM POLARIZATION
1.0
0.8
0.6
0.4
0.2
0.0
0°
20°
40°
60°
80°
90°
1/3 NORMAL
NORMAL
A=0
A=0.15
A=0.90
RAYLEIGH
(τ=0.1)
REFLECTED
φ=90°
TRANSMITTED
φ=90°
SOLAR ZENITH ANGLE

Fig. 19

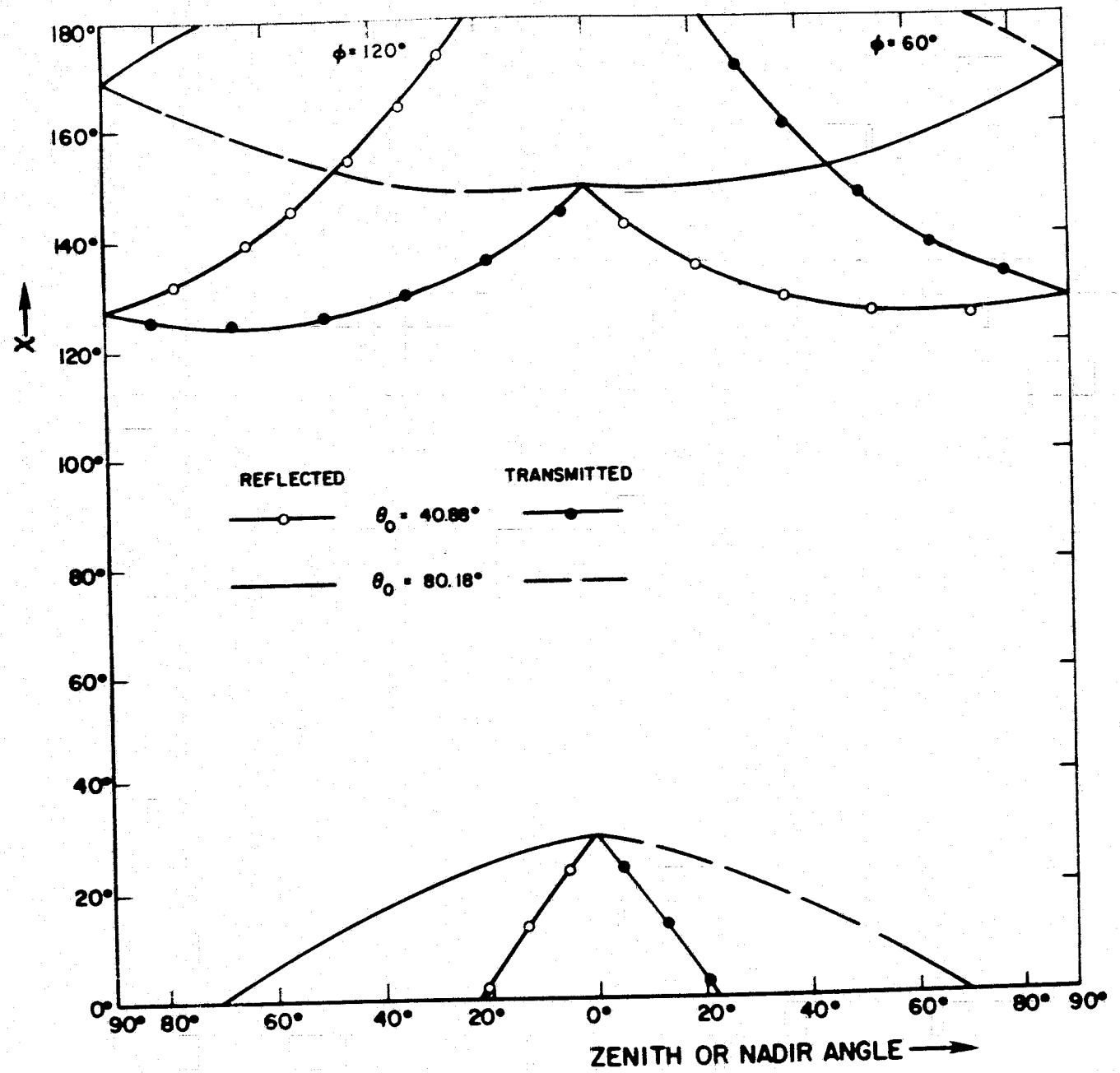
180°
160°
140°
120°
100°
80°
60°
40°
20°
0°
X
ϕ = 120°
ϕ = 60°
REFLECTED
TRANSMITTED
θ0 = 40.88°
θ0 = 80.18°
90° 80° 60° 40° 20° 0° 20° 40° 60° 80° 90°
ZENITH OR NADIR ANGLE

Fig. 20

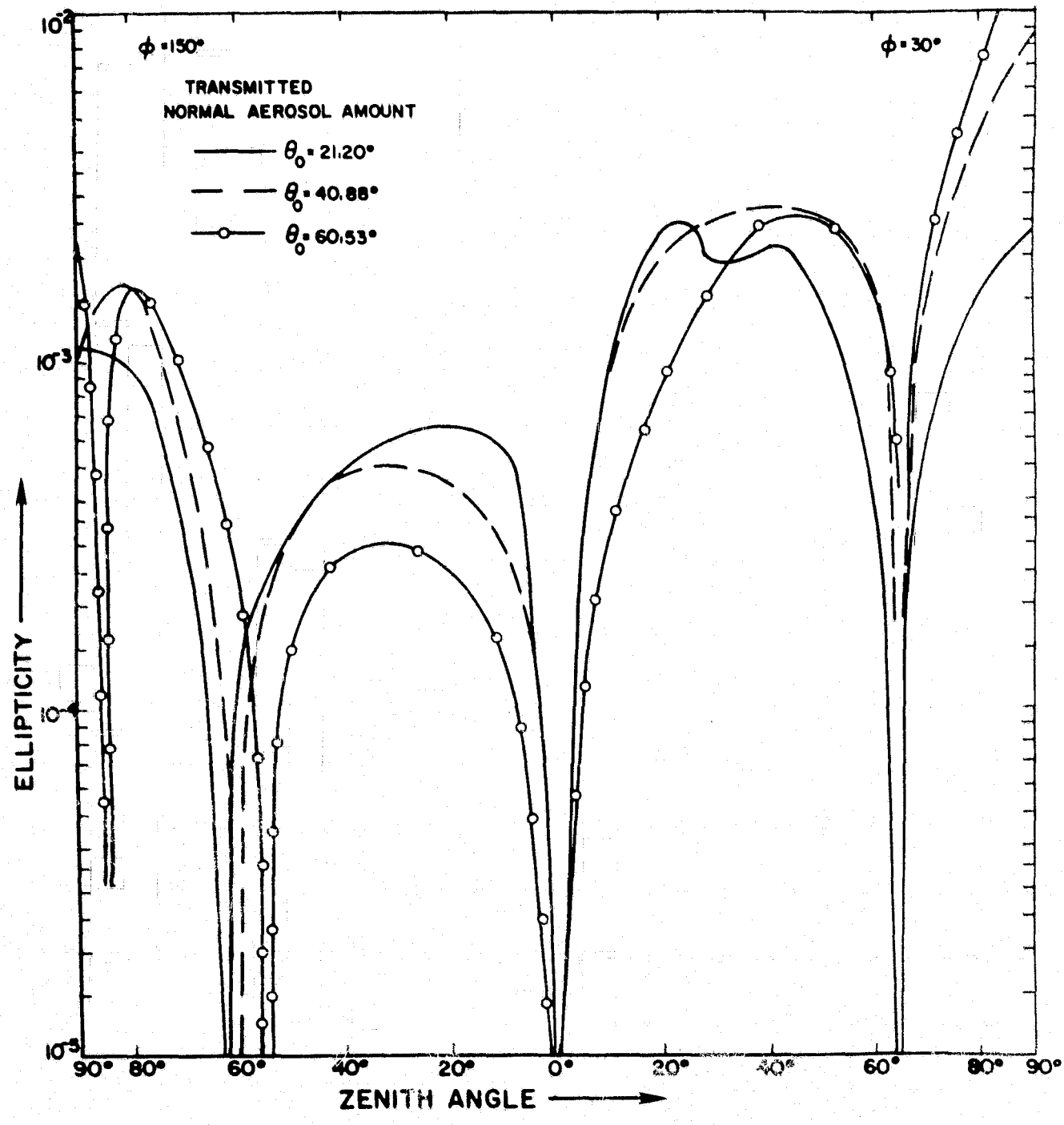
φ = 150°
φ = 30°
TRANSMITTED
NORMAL AEROSOL AMOUNT
θ0 = 21.20°
θ0 = 40.88°
θ0 = 60.53°
ELLIPTICITY
ZENITH ANGLE
90° 80° 60° 40° 20° 0° 20° 40° 60° 80° 90°

Fig. 21

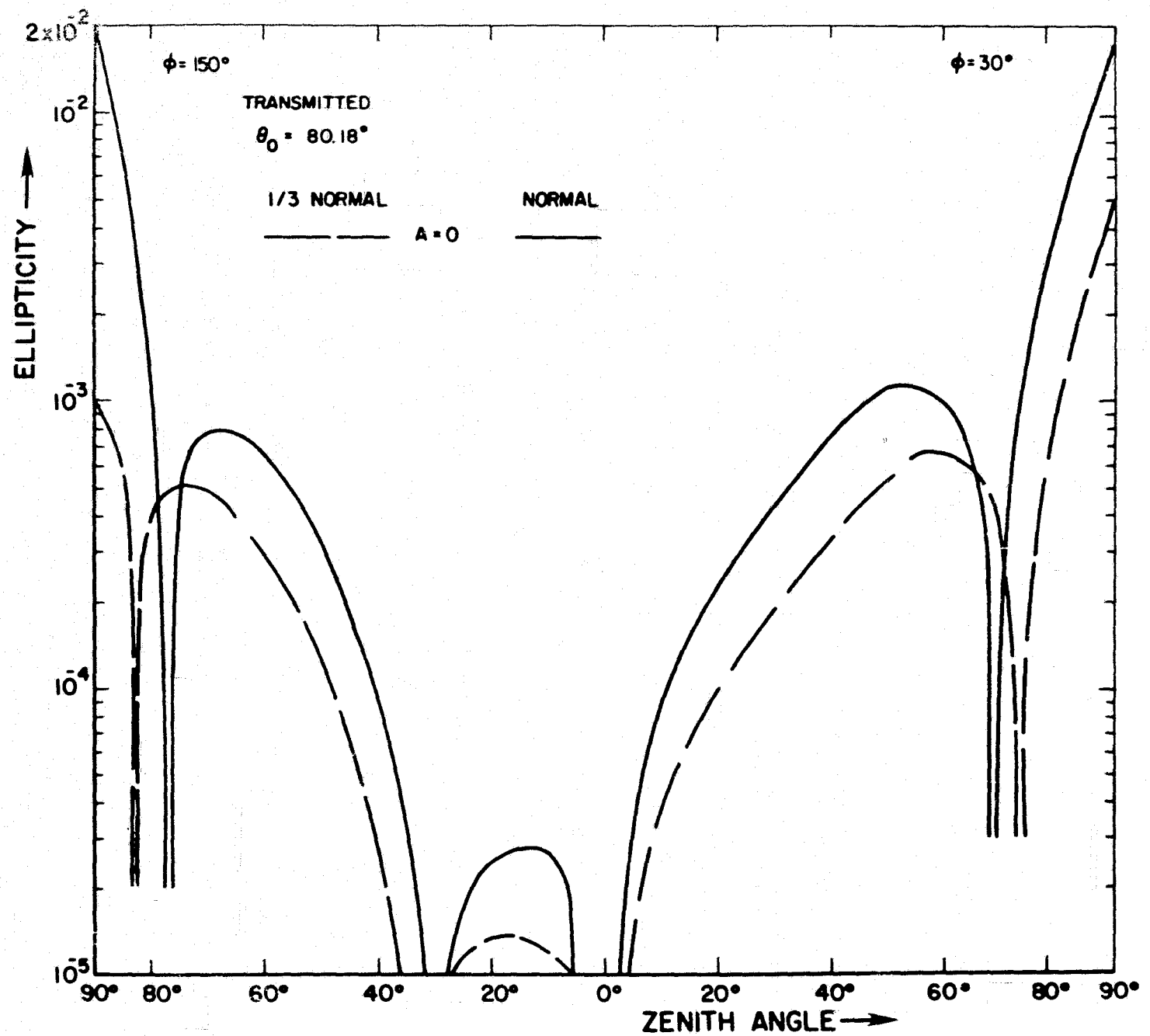
2×10^{-2}
10^{-2}
10^{-3}
10^{-4}
10^{-5}
ELLIPTICITY
$\phi = 150°$
$\phi = 30°$
TRANSMITTED
$\theta_0 = 80.18°$
1/3 NORMAL
NORMAL
A = 0
90° 80° 60° 40° 20° 0° 20° 40° 60° 80° 90°
ZENITH ANGLE

Fig. 22

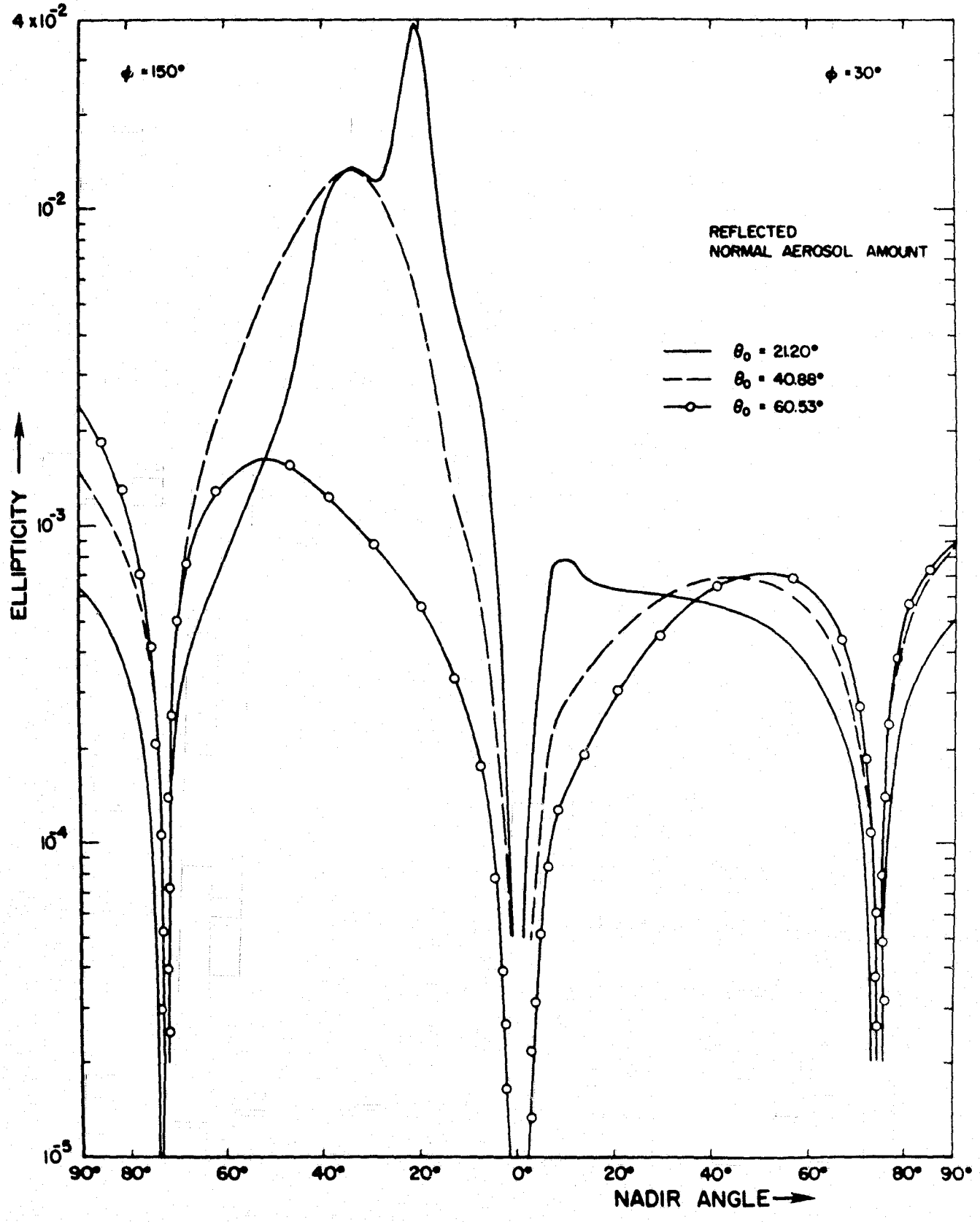
4 x 10⁻²
10⁻²
10⁻³
10⁻⁴
10⁻⁵
ELLIPTICITY
φ = 150°
φ = 30°
REFLECTED
NORMAL AEROSOL AMOUNT
θ0 = 21.20°
θ0 = 40.88°
θ0 = 60.53°
90° 80° 60° 40° 20° 0° 20° 40° 60° 80° 90°
NADIR ANGLE

Fig. 23

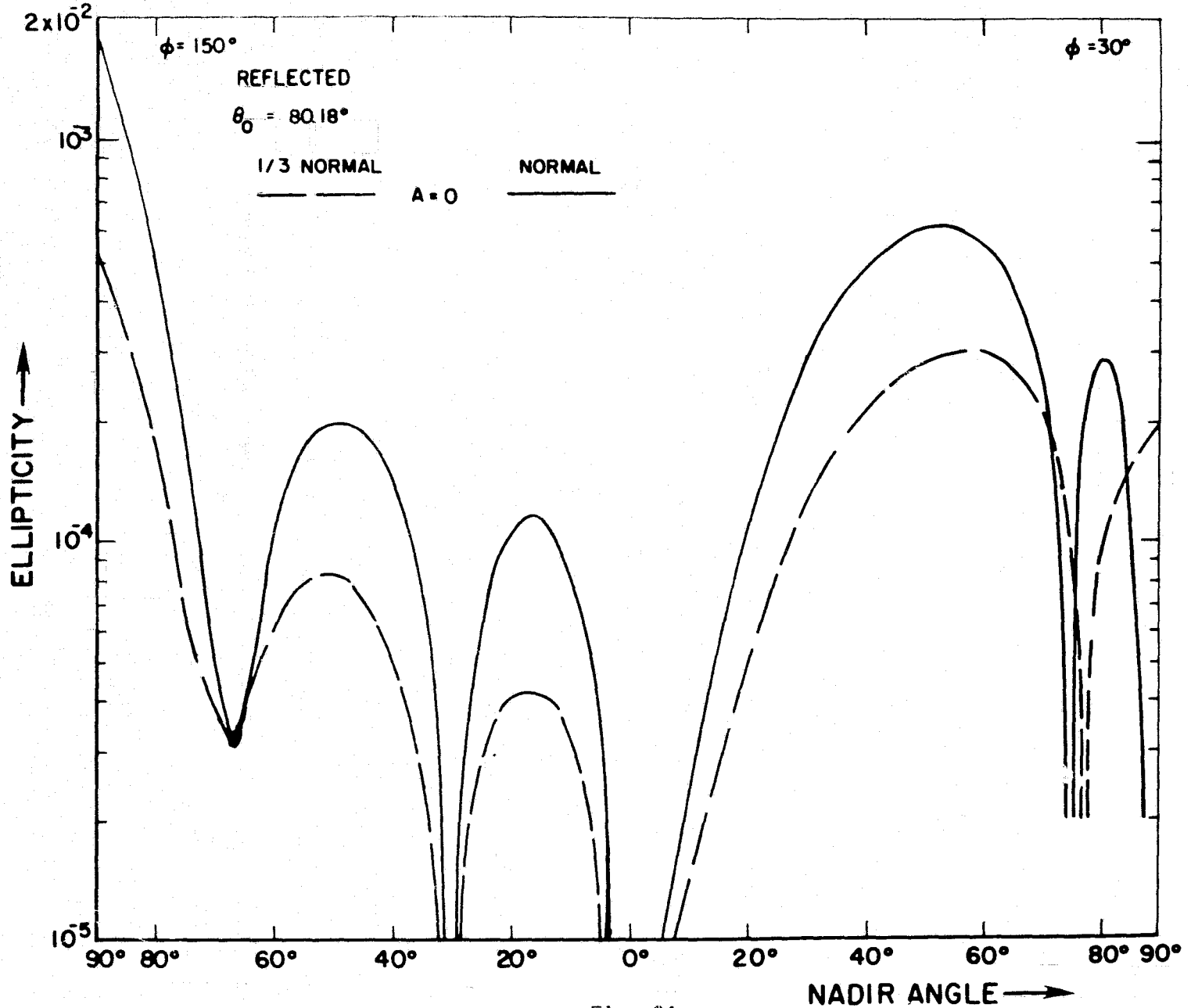
2x10⁻²
10⁻³
10⁻⁴
10⁻⁵
ELLIPTICITY
φ= 150°
REFLECTED
θ0 = 80.18°
1/3 NORMAL
NORMAL
A = 0
φ =30°
90° 80° 60° 40° 20° 0° 20° 40° 60° 80° 90°
NADIR ANGLE

Fig. 24